TÉCNICO LISBOA

Purification of a syngas stream for the production of hydrogen for fuel cell standards

Alessandro Pan

Thesis to obtain the Master of Science Degree in

Energy Engineering and Management

Supervisors: Prof. Francisco Manuel da Silva Lemos

Eng. Lorenzo Biacchi

Examination Committee

Chairperson: Prof. Maria de Fátima Grilo da Costa Montemor

Supervisor: Eng. Lorenzo Biacchi

Member of the Committee: Prof. Adélio Miguel Magalhães Mendes

November 2017

Acknowledgements

Thanking everyone for this achievement is hard, and I would like to thank everybody that helped me reaching this result!

I first would like to thank my parents, who always showed me an example to follow in my academic life, and motivation to go on in the studies and follow the topics that I liked the most; my sister Alice, who is always the wise support I need in hard times.

I would like to express any gratitude to my supervisor, Professors Francisco Lemos, for the useful hints and suggestions he gave me during the months of writing, and for his willingness of carrying on a thesis despite the long distance.

I would like to thank Innoenergy, for the wonderful organization they provide, and the experience of spending two years studying in different parts of Europe, which is something I find extremely positive for the development of the self and is as well valued in terms of career perspectives.

A special thanks goes to my friends, the old and the new ones, who I got to know during the past years traveling around Europe; a special mention goes to all friends of my old apartment in Lisbon, with whom I spent a valuable time of my life.

Last but not least, I would like to thank Cortus Energy, for the extremely enriching experience I had in this company, having a chance to gain a better understanding of several topics faced during my studies, while learning how they are applied in practice; now I can say I am really passionate about this field. I would like to mention overall Lorenzo Biacchi and Marko Amovic, for the example they give in the working environment.

Abstract

Climate change is a topic of increasing relevance in the last years, and the focus on new energy resources is fundamental in order to tackle it. Hydrogen has been defined as a promising candidate to replace fossil fuels in many areas, and its use is increasing at a rapid pace. Cortus Energy designs biomass gasification plants, with a patented technology named WoodRoll®, delivering a clean syngas which can be further upgraded to hydrogen for industrial and commercial use. This thesis has the objective of studying the purification of a syngas stream, produced through pyrolysis and subsequent gasification of biomass, in order to power a fuel cell system.

The possible purification systems are analysed in the State of the art section, and from the analysis of all the possibilities, the PSA – Pressure Swing Adsorption – is selected as the setup that best suits the technical specifications and setup of WoodRoll®, coupled with a Water-gas shift reaction. The concept of adsorption on solids is given and a theoretical and mathematical background is given on the phenomena of adsorption and the different theories that model it. An outlook on fuel cells and their current technological state is presented.

The possible setups are described together with the simulation run on the theoretical system; the simulations consider the variation of the cycle time, the gas composition and the adsorbent. The results are explained and commented in Chapter 5, together with a cost estimation of the unit and its P&ID.

Key words: Hydrogen, PSA, fuel cell, syngas

Resumo

A realidade da mudança climática global é um tópico cada vez mais discutido nos últimos anos, e o foco em novas fontes de recursos é fundamental para encarar o problema. O hidrogênio foi definido como um candidato promissor para substituir os combustíveis fósseis em diferentes áreas, e seu uso tem crescido a passos largos. Cortus Energy produz plantas de produção de gás a partir de biomassa, que usam uma tecnologia patenteada, chamada WoodRoll®. Esta tese tem por objetivo o estudo da purificação do fluxo de syngas advindo da pirólise e subsequente gasificação da biomassa para produzer hidrogênio para fazer funcionar um sistema de fuel cell.

Os possíveis sistemas de purificação são analisados em uma seção atingindo o estado de arte, e da análise de todas as possibilidades; o PSA – Pressure Swing Adsorption – é selecionado como método que melhor serve às especificações técnicas e forma do WoodRoll®, junto de um reator de inversão água-gás. O conceito de adsorção em sólidos é dado junto do contexto teórico e matemático sobre fenômenos de adsorção em geral e diferentes teorias que modelam esse problema. Um panorama sobre células de combustível e seu atual estado de desenvolvimento é presentado na fim do capitulo.

As configurações possíveis são descritas em conjunto com a simulação executada no sistema teórico; as simulações consideram a variação do tempo de ciclo, a composição de gás e o adsorvente. Os resultados são apresentados e comentados no capítulo da discussão, juntamente com uma estimativa de custo da unidade e seu P&ID.

Palavras chave: Hidrogênio, PSA, fuel cell, syngas

Contents

LIST OF TABLES

LIST OF FIGURES

LIST OF SYMBOLS

b	Adsorption equilibrium constant
C_i	Concentration of the gas [mmol/cm^3]
D_i	Diffusivity of the gas [cm^2/s]
d_p	Diameter of the particle [cm]
m_{ads}	Grams of adsorbent [g]
G	Gibbs free energy [kJ/mol]
H	Enthalpy [kJ/mol]
J_i	Flow of the gas *i* in a membrane [cm^3/cm^2·s]
k_a	Rate of adsorption constant
k_d	Rate of desorption constant
k_{ldf}	Linear driving force constant [-]
K	Henry's law adsorption equilibrium constant
K_0	Henry's law adsorption equilibrium constant at the reference conditions (T=298.73 K)
l	Thickness of the membrane [cm]
n	Number of moles
P_i	Permeability of the membrane in realation to the gas *i* [cm/cm^2·s·cmHg]
R	Universal gas constant, 8314 [J/kg·mol]
q_i	Amount of adsorbate *i* in the solid [mmol/g_{ads}]
q_m	Amount of adsorbate at the monolayer saturation limit
q_{max}	Maximum amount of adsorbate, at infinite pressure [mmol/g_{ads}]
q_s	Number of sites on the adsorbent
q_{sat}	Maximum amount of adsorbate charged on the adsorbent [mmol/g_{ads}]
Re	Reynolds number
S	Enthalpy
S_i	Solubility of the gas *i* in the bulk membrane [cm^3/cm^3·cmHg]
T	Temperature
u	Velocity [m/s]
V	Volume [m^3]
z	Axial coordinate in the reactor
ε	Porosity of the material [-]
ΔH	Change in enthalpy
ΔH_0	Change in enthalpy at the reference conditions (T=298.73 K)
ΔP	Differential pressure
θ	Fractional coverage
μ	Dynamic viscosity of the gas [Pa·s]
ρ_g	Density of the gas
ρ_s	Density of the solid

LIST OF ACRONYMS

AC	Activated Carbon
CHP	Combined Heat and Power
CMS	Carbon Molecular Sieve
LDF	Linear Driving Force
PEM	Proton Exchange Membrane
PSA	Pressure Swing Adsorption
QSS	Quasi Steady-State
SAE	Society of Automotive Engineers (USA)
SEK	Swedish Krona - Currency
TSA	Temperature Swing Adsorption
USD	Dollar of the United States - Currency
VPSA	Vacuum Pressure Swing Adsorption
WGS	Water-gas Shift reaction

1. Introduction

1.1 Background

In the past decades, the interest around environmental themes has become more and more a common topic of discussion, among people, industries, and governments. The amount of energy generated by renewable systems has increased sharply, to the point that in many countries, wind and solar power are not just a small figure, but they constitute a relevant component of the energy mix. Attempts of reducing global emissions have been made both at a European and world by Europe 20-20-20 and the Paris agreement signed in 2015. The exploration of alternative fuels has its roots during the energy crisis of 1973, in which the extensive exploitation of fossils resources was first taken into discussion. To be considered as significant, an alternative fuel has to be technically feasible, economically competitive environmentally satisfactory and readily accessible [1]. Hydrogen is the most abundant element in the universe, composing 90% of its atoms and more than 70% of all its mass [2].

Hydrogen has been extensively explored as one of the possibilities for energy generation and for industrial processes, because of its high specific energy content and the fact that its oxidation has a very high energy yield and produces only water vapor. However, due to the technical problems that arise from the use of hydrogen when compared to more easy-to-handle fuels, its use has been restricted mainly to the chemical industry where it is an important reactant in processes like the synthesis of ammonia or hydrotreating of oil fractions. There are now the premises and the perspectives of expanding its use in many other fields of use, especially in the long run. The businesses involved in hydrogen are currently relevant, as the worldwide production is around 65 million tons per year [3]

Hydrogen is a common element in the process industry, and its use is increasing. The main fields of application of this element are in the petrochemical processes, in the fertilizers production industry, in food processing, and in the energy generation industry. The latter use is developing just recently, thanks to a decrease in capital cost for fuel cell production and the use of these systems in functions such as backup power. Fuel cells are a strong candidate for the future of mobility, especially regarding heavy transport. When compared to electric cars, they overcome the problem of battery recharging times, as a hydrogen tank can be filled in few minutes. Hydrogen, in order to be sold for vehicle fuel cells standards, has to present very high levels of purity, higher than the purity required for stationary applications.

Hydrogen can be produced in different ways; currently, the cheapest and most common production process is through natural gas reforming or coal gasification. However, these processes emit CO_2 and use fossil fuels. An alternative way of hydrogen production is through biomass; in fact, biomass contains a considerable molar amount of atomic hydrogen. Hydrogen as a molecule can be produced both by biochemical and thermochemical routes; through steam gasification, the amount of hydrogen can be increased to an even higher level compared to traditional gasification processes albeit at the expense of added energy input. Hydrogen comes out of the process with many other gases – mainly CO, CO_2 and CH_4 in a varying percentage. It needs to be further processed in order to use it as a feedstock for other reactions or final uses.

The shift to a “Hydrogen Economy” is a topic that has intrigued many science disseminators and has first appeared in the literature in 1970 [4]. The main concept of this vision is the replacement of fossil fuels with hydrogen in all the main economic activities, and especially automotive industry. The shift to hydrogen as a way of fueling vehicles consists in a shift of energy carrier: hydrogen has to first be produced and only then can be used as a feedstock.

1.2 Aim of the thesis

This thesis has been developed during an internship at Cortus Energy, a Swedish company founded in 2006 that designs biomass gasification plants. The main goal of the company is to provide cost-effective renewable energy gas for power, industrial and transport applications based on the WoodRoll® system, the patented process that makes the technology unique and particularly suited to produce gases of high quality.

The feature that allows the gas to be very clean, and defined as “beyond the state-of-the-art” by external evaluators, is the fact that the processes of pyrolysis and gasification are separated: once the char is produced in the pyrolysis unit, it is ground to small size and injected into a gasification reactor; this allows to have a very small amount of tars and undesired pollutants in the resulting syngas. There are realistic perspectives of using the syngas produced by the WoodRoll® process for the upgrading of the syngas to commercial products, such as methane production or metallurgical biocoke.

The WoodRoll® system can process several types of biomass. Extensive testing has been done with the goal of learning to handle low-grade fuels at the test plant in Köping (Sweden). The composition of the syngas varies according to the type of feedstock that is used to power the system, resulting in different ratios of energy distribution between the pyrolysis gas and the carbonaceous matrix that is later gasified [5].

This thesis has the objective of studying a purification system for the syngas stream in order to produce hydrogen; the dry syngas contains about 60% of hydrogen. The objective of the full project, that goes beyond the scope of this thesis, is to commission a test system that can refine the gas up to the fuel cell specification purity. In the case the project is economically and technically feasible, this setting will be implemented in the testing plant of the company in Köping, Sweden, foreseeing the possible future application in a bigger commercial plant of 6 MW power.

1.3 Thesis structure

This thesis will be composed of three main sections that will first describe the problem under consideration and later present the solution that has been investigated. The main chapter of this thesis are:

- State of the art of syngas upgrading and purification
- Simulation of the systems
- Results of the simulations
- Discussion
- Conclusions

The first section is a state of the art review, in which the current technology used in similar systems involving the presence of syngas or reformate gas is described. The relevant chemical reactions, adsorption systems and the principles of adsorption technology are presented. The different systems that can be used for syngas upgrading are compared, and the working principles of a PSA unit are explained. A review on fuel cells and the purity that needs to be reached by the commercial hydrogen will be given.

Secondly, a model will be developed on the system selected: different simulation runs will be run on the model by changing parameters such as the gas composition, the type of adsorbent and the duration of the cycle. The equations used to develop the model and the method used to solve the system of partial differential equations are given at the beginning of the chapter.

The results are collected in Chapter 4 as a group of tables; in Chapter 5, in the discussion, they are analyzed and commented. In the same chapter, a Piping and Instrumentation Diagram – P&ID – together with a budget estimation for the unit are presented

The work is summarized in the conclusions, with the final remarks given to the project. In the Annex, the P&IDs are reported as A4 images.

2 State of the art

2.1 Current situation in the hydrogen market

Hydrogen has been for a long time a valid candidate for energy generation, but it is just in the recent decades that its advantages have been brought back into the energy research. The first experiments with hydrogen as an energy vector date back to the late years of XVIII century, but the discovery of cheap forms of energy such as coal, in the XIX century, and oil, until the 70s, put this fuel in the shadow.

The energy crisis in the Seventies brought hydrogen back into discussion, and during the years immediately following the oil crisis in 1973 many groups started research projects on hydrogen. In the meantime, hydrogen has remained an important reactant in the chemical industry. The current production is based on large chemical plants, using in most of the cases steam reforming reaction, particularly of natural gas; about 40% of the hydrogen production of the US are used for on-site purposes. Most of the current hydrogen production capacity in the world is aimed at high-scale and high-pressure industrial consumers, such as petroleum refineries and fertilizers production companies.

Hydrogen is fundamental for a large number of reactions, such as hydrocracking or ammonia production in chemical plants, but also food hydrogenation processing that allows hydrogenating fats. Chemical processes in refineries and oil industry involve hydrogen in many different reactions, because of the vast number of molecules and of chemical species that need to be treated. Plants are designed in such a way that the feedstock is processed as efficiently as possible, using all the byproducts in other reactions, in order to minimize the energy waste. Hydrogen production from coal is another common option, which has a setup by many ways similar to the WoodRoll® process; the char is reacted with steam, which gives origin to a gas rich in CO and H_2. Hydrogen can alternatively be produced through electrolysis, but this process accounts for a small percentage of the yearly overall production because of the high electricity consumption.

The NREL (National Renewable Energies Laboratory) of the United States [6] has studied the levelized cost of production of the different systems and shown in Figure 1, considering the different components of the total cost, and defined the hydrogen produced from biomass gasification as the renewable technology that can be proved to be the cheapest in the future. Natural gas reforming and coal gasification are cheaper from the production point of view, but the CO_2 emission makes them less competitive in an emission-reducing scenario. The costs of these techniques suffer from the heavy connection they have with the prices of feedstock, that could show strong variations in the future. Hydrogen production from biomass is thus seen as a reliable and cost-effective choice.

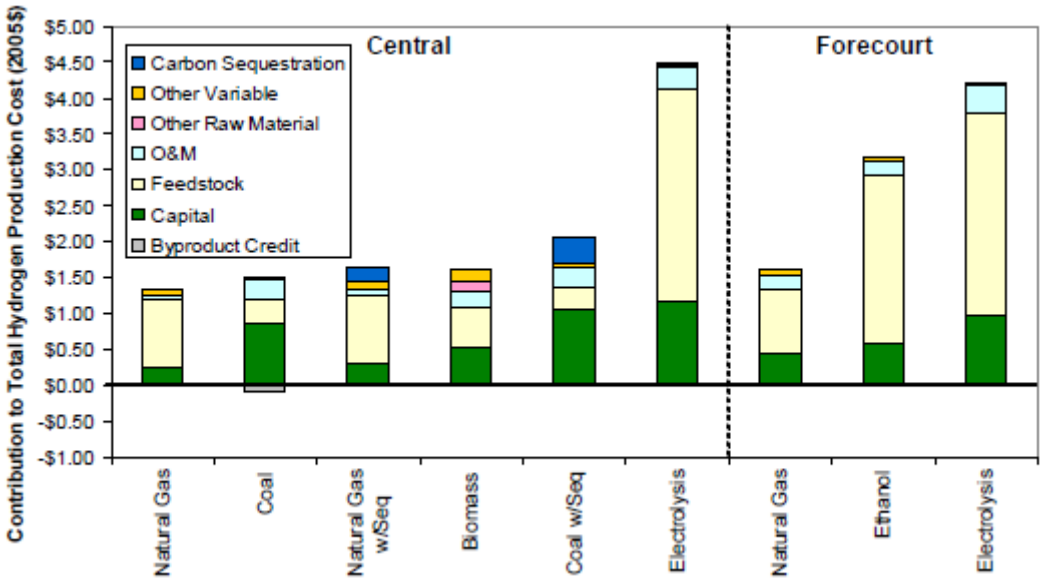

Figure 1. Levelized Cost of Hydrogen production, with different feedstocks [6]

The market worth of hydrogen is remarkably large: the total market of hydrogen, considering all the fields of application, was estimated to be 100 billion USD [7], while the global revenues for fuel cells and hydrogen for fuel cells were 5,6 billion USD in 2008 [8] and this figure could grow up to 38,4 billion in 2020. By 2019, there could be up to 700,000 job places directly connected to the hydrogen and fuel cells industry [8].

The study made by the NREL [6] considered two main different approaches for the production: a centralized one, with the production of at least 50,000 kg/day of hydrogen, and a distributed approach, which gives a range around 1500 kg/day. The advantage of the small-scale technology, as is the WoodRoll® technology, is that it meets the local needs of a community, and powers systems such as a refueling station or a centralized heating system. The objective to aim to at the moment of the publication of this article was to reach the cost of 2$/kg of hydrogen, before taxes. A major voice of costs in small plants is represented by the storage and compression costs, that make up about 1,90$/kg that sum up to the basic production cost.

2.2 Outlook on the upgrading methods

The process of producing hydrogen through a gasifier or a steam reformer involves the production of syngas. The gasification process produces a gas that also contains a significant amount of impurities that have to be removed before the syngas can be used for further applications. There can be different upgrading methods depending on the purity level required for the specific use. In the following subchapters are listed the most common industrial processes that can be used to produce a hydrogen-rich product gas. Water-gas shift reaction is a way of optimizing the system's production of hydrogen, by converting the CO into CO_2 and produce an additional quantity of hydrogen, in order to have an increased calorific value and composition, while other methods (PSA, membranes, and distillation) are separation techniques. A valid literature reference to study these processes in a deeper detail is the publication from 2010 "Hydrogen and Syngas production and purification technologies" [9].

2.2.1 Water - gas shift reaction

The water - gas shift reaction is a reversible and exothermal reaction between steam and carbon monoxide in order to produce hydrogen and carbon dioxide. The reaction takes places between a mixture of CO and H_2O, the main components of the syngas from coal or biomass gasifiers, and is:

$$H_2O + CO \Leftrightarrow H_2 + CO_2 \quad (1)$$

The advantages of using this process in a setup in which hydrogen is needed at a high purity in the downstream reactors are twofold: on the one side, the total flow of gas increases thanks to the injection of steam, which increases the energy use of the feedstock; on the other hand, the percentage of hydrogen contained in the mixture is increased. In the case of a PEM fuel cell system coupled with biomass gasification, a critical parameter to be considered is the poisoning of the catalyst because of the presence of carbon monoxide [10]. The syngas at the outlet of the gasifier contains about 25% of CO, which needs to be reduced by around 10 thousand times: for a proper working of the fuel cell, the maximum allowable concentration of CO for fuel cell application is stated to be 25 ppm. The amount of CO and other pollutants that can be withstood by a fuel cell will be discussed more extensively in the chapter regarding fuel cells.

Water-gas shift reaction is an exothermal reaction that is kinetically favored by elevated temperatures but thermodynamically favored by lower temperatures. Because of this reason, in the industrial practice, the usual layout is to have two stages of the reaction, separated by an intercooler; an example of the setup is shown in Figure 2. According to the feedstock type, there are different types of gas cleaning units. In the case of coal or biomass, a desulphurization stage is included in the system to get rid of the sulfur contained in the syngas.

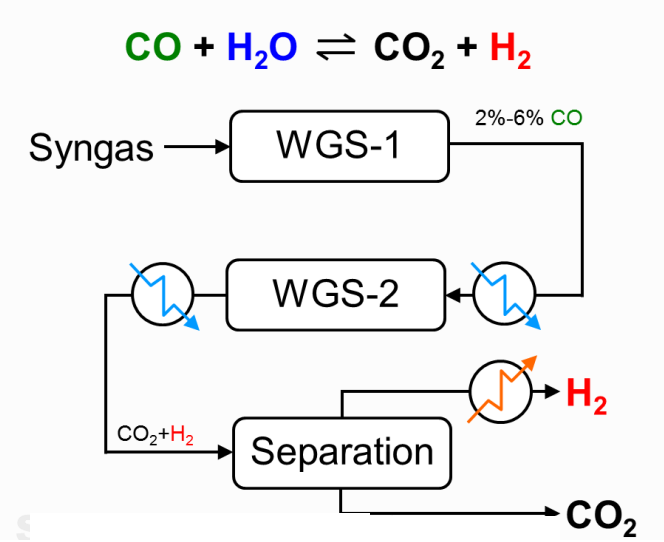

Figure 2. Scheme of the setup with two stages of WGS and a separation unit [11]

The position of the water-gas shift reactor is dependent on the conditions of the process in the specific case; when the water-gas shift reaction is used on a syngas that still contains sulphur, it is named “sour shift”, while in the case of performing the water-gas shift on prior desulfurized syngas, it is called a “sweet shift”. The choice between sour or sweet shift depends on the application and composition of the syngas. The effect of sulfur is

particularly important in the case of coal gasification, but since the WoodRoll® process applies only biomass-based fuels, the type of shift considered in this work is sweet.

The number of moles remains constant before and after the reaction, thus the equilibrium constant is almost not affected by the value of pressure. In industrial practice, this reaction is generally carried out under pressure so that the increased amount of gas is passed to the PSA without the need of a further stage of compression.

Several types of catalysts can be used to promote the water-gas shift reaction; different temperature ranges can also be used. A possible catalyst for the high-temperature shift is iron. The syngas, at a temperature that ranges between 350 and 550°C according to the feed composition, is mixed with steam on a chromium or copper promoted iron catalyst; the operating pressures are up to 30 bars. The first part of the shift is less sensitive to the pollutants contained in the stream; the amount of CO contained at the end of this stage is around 4%. At this point, there is an intercooling system and the temperature is lowered to about 260°C. The reaction of conversion of CO at this temperature is not favored from the kinetic point of view, but is enhanced from the equilibrium point of view; using the two temperature shifts is a way of taking advantage of both the kinetic and the equilibrium in the reaction. The catalyst in this stage is Cu/ZnO or CoMo.

Besides sulfur, particular attention has to be put on chloride, which is present in some particular types of biomass such as straw or rice: this element is poisonous to the copper catalyst and can lead to an earlier substitution of the catalyst; a safe amount is under 0.1 ppm [9]. Condensation has to be absolutely avoided, as it can be harmful to the catalyst: for this reason, the lower temperature limit is 200°C. The reactor presents an increase in temperature of about 15°C along the direction of the flow since the reaction is moderately exothermal.

There are other possible reaction technologies that are being developed, especially destined to vehicles and portable applications, in order to be able to power this electric equipment with a system made of a fuel processor together with fuel cells. Possible developments are [9]:

- WGS membrane reactors, able to produce hydrogen with fuel cell specifications
- Oxygen-assisted WGS that combines preferential oxidation with the water-gas shift reaction
- Intensification of the process in micro-channels for temperature optimization

2.2.2 Membranes

The use of membranes for gas separation is a practice that is commonly used in processes such as the biogas upgrading, in order to separate the different components of a mixed stream. This process is in most of the cases a pressure-driven separation process, located downstream to the reforming or the syngas generating reactions that generate a gas rich in hydrogen, carbon monoxide and carbon dioxide. The feed gas is separated thanks to the different ability of the molecules of permeating into a membrane; the properties of the gas, the properties of the membrane material and their mutual interactions are extremely important for this reason.

There are four main types of membranes, divided according to the composing material [9]:

- Polymeric membranes. They are the type of membrane that has seen a wide commercialization; they can be further divided according to the inner structure in asymmetric or composite.
- Porous membranes. They have experienced many development efforts in the recent period.
- Dense metal membranes. Very effective in the case a high purity of product hydrogen is needed, even with a single stage of compression.
- Ion-conductive membranes. Very little applied in the case of hydrogen separation.

The working principle of a membrane can be defined as a feed stream that enters the membrane module, and is divided into two different streams according to the composition of the feed gas and the permeability of the molecules in the feed gas: the higher permeability a gas has, the easier it will be for it to pass through the membrane. The usual appearance of a membrane module is cylindrical, or in some cases, rectangular. The stream flows in the axial direction, while the permeate passes through the membrane in the radial direction; the basic scheme is shown in Figure 3.

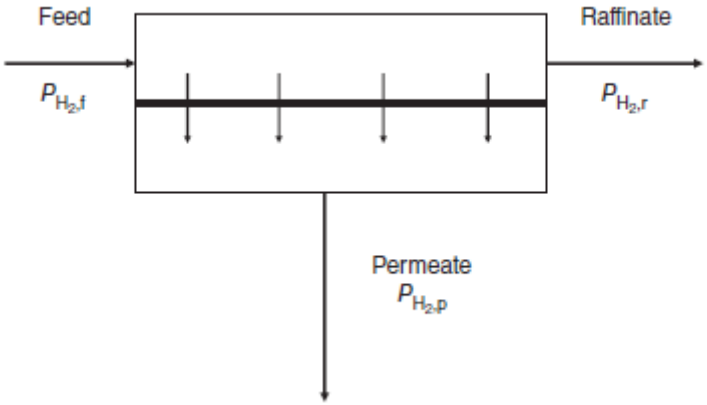

Figure 3. Working scheme of a membrane **[9]**

The flow of gas that characterizes each stream is defined by J_i, and it is a function of the membrane thickness *l*, the differential pressure, and the permeability *P*:

$$J_i = P_i \frac{\Delta P}{l} \tag{2}$$

While permeability is defined as the product of diffusivity of the gas in the bulk membrane *D* by the solubility of the gas in the permeating membrane *S*:

$$P_i = D_i * S_i \tag{3}$$

The other important parameter to be considered for the choice of a membrane for hydrogen separation is the selectivity, which is the ratio between the permeabilities of two components of the mixture. Ideally, to have a perfect pure product stream, the selectivity should be infinite. The metal membranes, in proper conditions, actually have infinite selectivity with hydrogen.

These factors are mutually connected, and ideally, a membrane has a high flow, a high selectivity and a high recovery, which is the percentage of the amount of the useful component (in this case hydrogen) that is present in the output gas. The economic logic would likely be to have a recovery as high as possible, but this fact leads to a reduction of the differential pressure and to an exponential increase in the area of the membrane, increasing by far the capital cost of the unit.

Different types of membranes have different behaviors in the parameters that have just been shown. For example, nanoporous membranes allow a relatively high flux, but the selectivity is in general low. For fuel cells application, dense metal membranes offer excellent parameters. In fact, the mechanism of diffusion of hydrogen is such that an extremely high selectivity can be achieved. The dense metal membrane is constituted by metals such as palladium or palladium alloys, and metals of groups 3 and 5; an important parameter to be taken into consideration is to avoid the embrittlement and the contamination by the other components of the syngas stream such as sulfur.

The hydrogen molecule is split into two atoms, that bond to another atom in the metal bulk and, through diffusion, they migrate through the membrane. Thanks to this fact, a very high purity can be achieved even with a single pass, while polymeric membranes need at least two passes, with a higher cost for the double stage of compression; to give a grasp of the difference of selectivity between hydrogen and carbon monoxide, a polymeric membrane can achieve usually 200 fold concentration, while a dense metal membrane produces concentration enhancements in the range of 100,000 [9]. Together with a higher purity, there is a substantially lower amount of trace contaminants in the purified stream.

An advantage of membranes is that their capital cost is almost proportionally linked to their area; moreover, their operation is relatively simple. Because of this reason, their use is particularly interesting in the case of small-scale applications, such as small reformate streams purification, in which the capital cost and the operational issues of other purification methods would be problematic.

Dense metal membranes are not selected as a possible upgrading method for the syngas produced by the WoodRoll©. Even though in laboratory test they have very good performances, the development stage of dense metal membranes is not developed enough to be applied the particular context that this work is considering.

2.2.3 Cryogenic distillation

Cryogenic distillation is a process that is based on the different liquefaction temperatures of the gases composing the syngas and allows to separate the hydrogen in a straightforward way thanks to the very low liquefaction temperature of this gas, which is just 20 K. The other components of the stream, such as nitrogen and carbon dioxide, will liquefy at higher temperatures and can be separated.

The main drawback to this technology is, despite the simple theoretical principle, the complexity of operation. The process is very highly electricity-requiring in comparison to other technologies, and for this reason, it has

been gradually abandoned. Another issue occurs when there is water vapor present in the feed gas that causes blocks in the compressing unit due to the formation of ice.

Despite these limitations, cryogenic distillation is a common system of separation in the case of CO_2 production, especially from feedstocks with an already high CO_2 concentration, as it allows the direct production of liquid carbon dioxide that can later be sold. In the case of hydrogen production from syngas, it has been replaced by other more efficient methods such as PSA or membranes in the past decades. Due to this specific field of operation, the use of distillation for hydrogen production is not common, and will not be further investigated for the application in the purification system.

2.2.4 The PSA unit and its main cycles

Pressure Swing Adsorption is a common method of gas separation, hydrogen purification, and gas drying. The basic concept behind it is the property of a molecule from a fluid phase to be bonded through intermolecular forces; since this property varies strongly according to the type of gas and the environmental conditions, these parameters are varied in order to achieve different types of separations.

The following chapter will go through the physical properties that allow adsorption to be possible and will make a quick outlook on the other possible types of adsorption used in industry. There will be as well a study of the different materials used in the units, and the gases that can be purified with this system.

The amount of gas adsorbed is a function of the pressure and the temperature; in such a way it is possible to design a cycle that allows varying the environmental conditions, and selectively adsorb or desorb one of the components of the gaseous stream. The difference between the PSA and TSA is shown in Figure 4 on a plot that correlates the loading of a material with its partial pressure (isotherm). The physical phenomenon that is used by this type of process is the selective adsorption in the solid material of one or more components of the gas, allowing the other passing through.

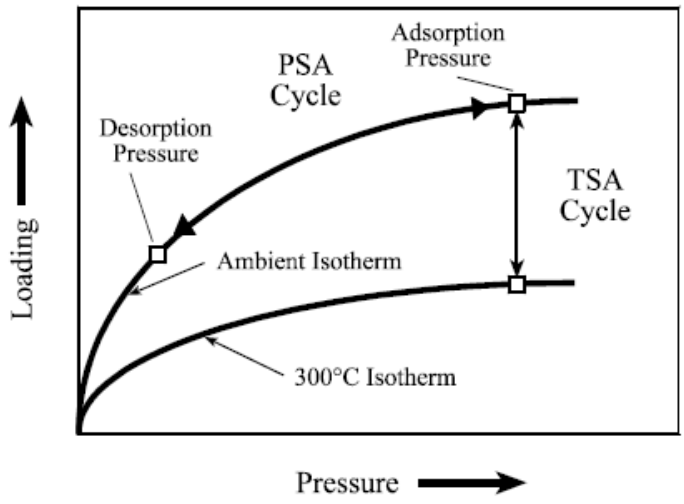

Figure 4. Schematic of the working principle of PSA and TSA

There are two different types of adsorption cycles that are defined as pressure or temperature swing adsorption; the choice of one or another is dependent on the particular conditions of the problem, and on the characteristics of the gas to be treated. In general, temperature swing adsorption is a more energy-consuming process, takes more time, and thus requires a bigger reactor; however, it is a possible choice in the case there is the waste heat that can be used in the process. An analysis for the choice of one of the systems for the case of hydrogen purification in refineries has been done by Golmakani in 2016 [12]. Since the system that is planned to be purchased is small and there is no availability of waste heat, the author has decided to focus only on the application of PSA to the case.

The PSA is a separation technique that has been developed more than 50 years ago and it is widely known and applied in industrial practice. The first attempt of concentrating a gas through the variation of pressure has been done in 1930 by Finlayson and Sharp, with a single column. The following development has been done by Skarström in 1960 [13], considering a basic cycle made of four steps, and using two different beds, in order to increase the efficiency and the recovery.

The simplest cycle, as first designed by Skarström, consisted of four steps:

1. Pressurization. The bed column is pressurized with the inlet of feed gas
2. Adsorption. The valve at the outlet of the bed is open and the feed gas is let flow in the column
3. Depressurization. The column pressure is gradually reduced, letting out the gas
4. Purge. The column is purged using a part of the gas produced by the feed

The cycle is referred to a single column, but it can be applied to many different columns simultaneously. With the developments of the research on this topic, the design of cycles has become more and more complex, adding different columns and increasing the efficiency and the complexity of the system. The systems are usually designed in such a way that there is always a column that is accepting feed gas, in order to have a continuous flow of purified gas. In Figure 5 is shown a basic Skarström cycle.

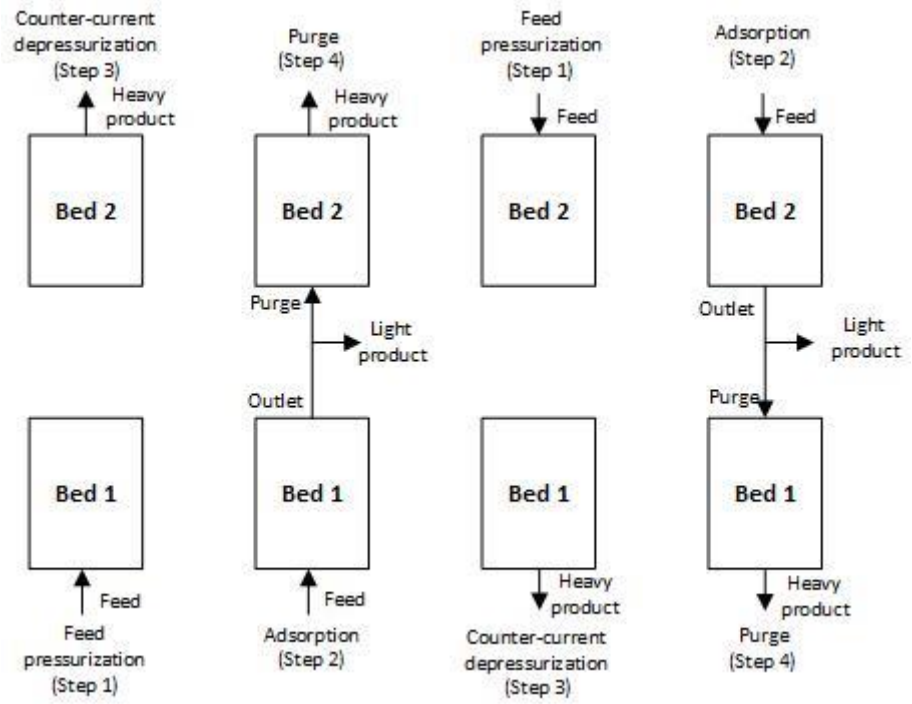

Figure 5. Example of a Skarström cycle for a two-bed system

The number of beds of a PSA system can vary greatly: there are examples of PSA systems with a single bed [14] and multiple beds; in general, the common practice in industrial systems is to have many different beds, up to 10 or 12, since the flows that can be treated are measured in thousands of cubic meters per hours. This is quite typical in refineries that are one of the main fields of use of PSA: the size of these plants is extremely big.

Increasing the number of beds and process steps, the total efficiency of the process increases since parameters such as the energy for compression and the utilization of the adsorbent are increased, thanks to more equalization steps and the use of co-current and counter-current flows. This upgrading is, of course, easier in major plants compared to the small units; in Figure 6 is reported the Polybed process.

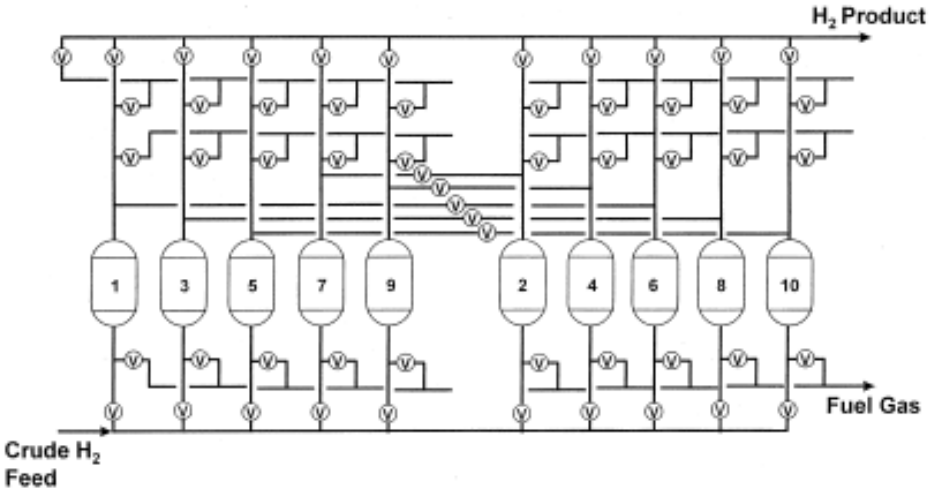

Figure 6. Example of an industrial PSA (Polybed process)

The main cycle design consists of four main steps, but in the case of real systems, the configuration can be optimized in many different ways. As it has just been said, a common practice is to save compression energy for the pressurization of a bed thanks to the use of waste gas from another bed; more developed systems such as the Polybed process (figure 4) use a combination of co-current and counter-current phases, in such a way that the adsorbent is used in an optimal way. The performances of such systems can be very high: for example, the 10 beds system shown in figure 4 could refine an off-gas composed of 77.1% H_2, 22.5% CO_2, 0.35% CO, 0.013% CH_4 into a stream with 99.999% H_2 and a recovery of 86% [15]. The achievement of this technology, patented by UOP in 1976, is that the capacity of the plant is potentially unlimited since more beds can be connected at once to the feed. Because of this reason, the PSA technology became more and more popular in the petrochemical industry.

While the first PSA design allowed only to recover one of the components of the stream, the research done on the topics allows now to separate the stream into two or more sub-streams, thus allowing to compact multiple units in one system. Another important technological introduction was the purging step done at under-atmospheric pressure: by connecting the system to a vacuum pump, the desorption pressure is a fraction of the atmospheric and the desorption is quicker and more effective [16].

2.3 The concept of adsorption

Adsorption is the phenomenon described by the bonding of molecules from a fluid phase on a solid surface. This bonding is caused by several types of intermolecular forces, either strong or weak, grouped in the general categories of chemical bonds, or the result of many weak intermolecular forces. Adsorption is defined as a surface phenomenon [17], as the interactions that happen on the surface of the material are not affecting the behavior of the bulk of the solid; Adsorption is widely present in many natural, biological, physical and chemical systems, as well as in many industrial applications. It is distinguished from the case of sorption of a gaseous molecule inside the bulk of a liquid: in that case, the process is named “absorption”.

Adsorption refers to the net accumulation of a chemical species at the interface between a solid phase and a fluid phase, leading to a loss of one or more species from the latter [18]. It is a consequence of the different energy levels connected to the bonds of the surface molecules in comparison to the bonds inside the bulk of the solids. In fact, as it is possible to notice as well from empirical experience, surfaces are more reactive than the bulk; surface energy is a characteristic of the solid state that can be defined as the energy required for the disruption of bonds when a surface is created.

Since the molecules located on the surface of the solid do not have all their bonds occupied by the neighboring molecules, they are at a higher energy level and are more prone to form bonds with external molecules more than with the internal. The fact that the molecules located in the bulk are at a lower energy level compared to the ones located on the surface has a physical proof: otherwise, there would be a driving force removing the molecules from the inside towards the outside of the solid. There are two distinct regions in the interfacial layer: the surface layer of the solid adsorbent, and the adsorption space, in which the enrichment of the adsorbate

takes place [19]. Figure 7 shows how a simplified version of the intermolecular forces of atoms on the surface and in the bulk of the solid; the forces of the surface atoms are not balanced in all the directions.

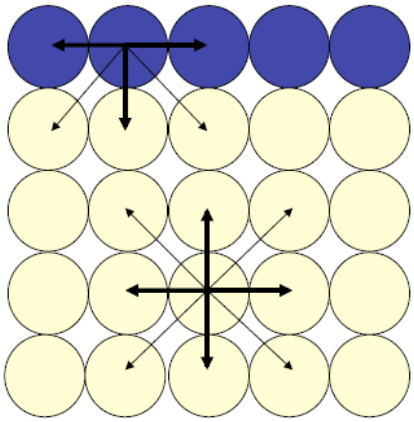

Figure 7. Representation of the intermolecular forces between molecules in a solid [20]

Adsorption is always an exothermal reaction since it is associated with the reduction of the entropy of the adsorbate that thus releases energy. From the thermodynamic point of view, the Gibbs free energy states the maximum reversible work that can be done at constant temperature and pressure [21]:

$$\Delta G = \Delta H - T\Delta S \tag{4}$$

This formulation states that for a process to be spontaneous the variation of free energy should be negative. Since the variation in entropy is negative too, it follows that the variation in enthalpy must be negative and heat is thus released. Adsorption is exothermal, which in the case of adsorption is an unfavorable effect. The equilibrium position of the process is gradually shifted to the desorption side in the case of an increase in temperature and, as the opposite effect, adsorption is enhanced by colder temperatures while the material is let out of the solid matrix.

The solid that is used to perform this process is named “adsorbent” and can have very different compositions and structures; a critical parameter for adsorbing materials is their specific area, as adsorption is a surface phenomenon, which is often connected to porosity. Although in many cases porous materials are chosen for their adsorptive properties, non-porous materials can be used as well, such as non-porous nanoparticles. The size of pores is a characteristic of the adsorbent material, which is chosen according to the properties of the fluid to work on. As far as applications are concerned, the requirements for an adsorber are that it needs to present high selectivity, capacity and lifetime [22]. Adsorption materials can be classified into inorganic, organic and hybrid adsorbents. The main class of adsorbents that matter with the purposes of this work are inorganic, so the work will be more focused on this type of substances.

The fluid that is attracted by the solid surface is defined as “adsorbate”: its molecules bond to the surface of the adsorbent, eventually creating a layer on the surface of the adsorbent. The ways of depositing on the surface are different and depend on the type of adsorbent and adsorbate: there are different mathematical models that

have been developed to describe these interactions [23] that will be described in Chapter 3. The rate and the ease of this process depend strongly on the type of material and on the type of gas; during this chapter, these possible settings will be analyzed.

The behavior of porous solids of adsorbing large volumes of vapor was first noticed during the XVIII century by the scientists Scheele and Fontana [24], and the industrial practice of using this principle for industrial purification of gases has been developed from then on, and especially during the last century. The phenomenon of sorption of a gas into another phase has been studied by the English chemist William Henry, that formulated the widely known "Henry's law" that constitutes the simplest way to describe how a gaseous compound can be absorbed in a liquid [25]; it will be explained in this work how the phenomenon of adsorption between a fluid and a solid can be explained using this theory. The main processes in which adsorption is used are categorized into purification processes and separation of a mixture into components. The difference is that in the first case a component with small economic value is isolated from a more valuable component which is later used or sold, and in the latter, both the components have a practical value and are not discarded [22].

Adsorption is a common phenomenon that is not only industrial but is as well present in everyday life. For example, it allows the paint to stick to the surfaces, by building chemical and mechanical bonds with the surfaces; adsorption makes possible to purify drinking water in filtering carafes, retaining the polluting elements in the filter.

2.3.1 Empirical and chemical models

There are different models of adsorption that are divided into two main groups: the empirical models and the chemical models. The first ones describe adsorption data and are often based on the extrapolation of the behavior of a phenomenon according to the real observations and then use it to produce analytical correlations; the latter provide a molecular description using the chemical equilibrium approach [23].

Chemical models are often explained with surface complexation models; complexation models calculate the values of thermodynamic properties mathematically, by treating ion adsorption as a complexation reaction in a solution. A complexation reaction is a process that involves a central ion (usually a metal) that links to other molecules, in a number of bonds superior to its coordination number; this is possible because of the weaker nature of this type of connections.

The analysis this thesis considers the use of empirical data, taken from adsorption curves for materials that have already been tested and studied.

2.3.2 Chemical adsorption and physical adsorption

Adsorption is divided into two main categories that are named physisorption and chemisorption. This classification is done according to the fact that the interaction between the fluid and the solid is mainly physical or chemical, which in other words means investigating whether there is the interaction of a covalent bond between molecules, or just an intermolecular force tying the molecules to each other [26].

Chemical adsorption, or chemisorption, occurs when the adsorption process involves the formation of chemical bonds and is thus stronger than physical adsorption: the molecules of fluid undergo a chemical reaction with the surface of the adsorbent and bond to particular sites on its surface. This situation presents a high energy release, which is the energy connected to the formation of molecular bonds (named heat of adsorption); it depends heavily on the adsorbent characteristics and on the target fluid. The heat released in chemical adsorption is higher, and in some industrial applications, it needs as well external cooling.

Physical adsorption, on the other hand, is characterized by the attraction of fluid molecules to the surface of the pores of the adsorbent; the driving forces are the van der Waals forces and usually have a low heat of adsorption, with an energy comparable to the latent heat of sublimation of the adsorbate. The bonding forces are relatively weak, thus the amount of energy needed to desorb the gas is lower as well. Figure 8 shows the distinct levels of potential energy connected to chemical and physical adsorption, in relation to the distance to the adsorbent molecule. The fact that chemisorption involves the sharing of an electron makes possible that the mutual distance is lower and the potential energy of the bond is higher.

Figure 8. Scheme of the potential energy related to adsorption

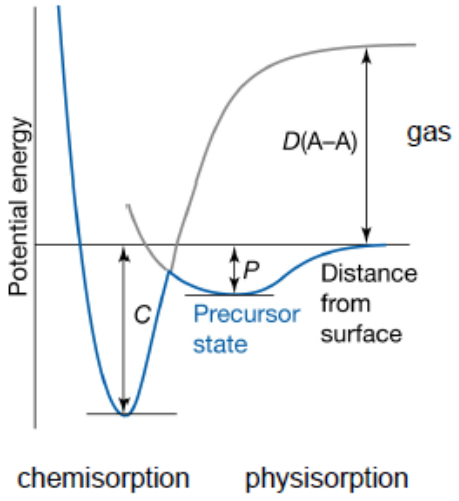

Figure 8. Scheme of the potential energy related to adsorption [20]

To make an example, adsorbing carbon dioxide with activated carbon (case of physisorption) releases less than half the energy released using an amine (case of chemisorption) [26]. The presence of chemisorption means having a higher removal capacity at lower concentrations: thus it is an important way to remove traces of contaminants [20]. The bonds can be created between the adsorbate and the adsorbent, but not between the molecules of adsorbate; this means that just a single layer of molecules can be formed, and chemisorption is almost always restricted to a monolayer and the capacity per unit area is much more limited than in some cases of physisorption where multi-layer adsorption or even pre-condensation phenomena can occur.

Physisorption and chemisorption have different adsorption times, noticeably different in the two cases. This figure varies, in fact, between the range of an extremely small fraction of a second for physisorption to up to

tens of seconds in the chemisorption region, depending on the kinetics of the reaction involved. The meaning of this fact is that in the case of physical adsorption there is a continuous and rapid movement of particles between the solid and the fluid around, while in the chemical adsorption there is a rearrangement of the molecules on the surface, which takes more time [22].

According to the type of process that is desired to perform, it is necessary to carefully choose the type of adsorbent in order to have the most suitable reactor, according to size, cost or energy consumption. In general, chemisorption in commercial applications is connected to bigger amounts of reactants, and thus requires higher amounts of equipment and investments and it also requires higher amounts of energy for the desorption stage. Considering the previous example, solid amines are a well-working chemical adsorber for carbon dioxide removal; the drawback is that a high energy amount is required for its regeneration and the solvent is not simple to handle. For these reasons, the system is not suitable for small applications because of plant complexity and cost [27].

A summary of the differences between chemisorption and physisorption is provided by Ruthven, in his work "Principles of Adsorption" [22]; it is reported in Table 1.

Table 1. Summarization of the differences between chemisorption and physical adsorption **[22]**

	Physical adsorption	**Chemisorption**
Heat of adsorption	Low: 2 or 3 times smaller than heat of evaporation	High: 2 or 3 times more than latent heat of evaporation
Selectivity	Non-specific	Highly specific
Physical characteristics	Monolayer or multilayer. No dissociation of adsorbed species. Only significant at relatively low temperatures.	Monolayer only. May involve dissociation. Possible over a wide range of temperatures.
Type of bonds	Rapid, non-activated, reversible. No electron transfer although polarization of sorbate may occur.	Activated, may be slow and irreversible. Electron transfer leading to bond formation between sorbate and surface
Influence of temperature	Decreases with temperature increase	Increases with temperature increase

It is as well remarked that the vast majority of separation processes depend on physical adsorption rather than chemisorption, thus the focus of studies related to this topic is generally more focused on physisorption rather than chemisorption.

2.4 The adsorption isotherm

The adsorption characteristics of a material in relation to an adsorbate are expressed with diagrams named isotherms. These diagrams represent the amount of adsorbate in the adsorbent (represented on the y-axis) as a function of the partial pressure of the adsorbate (on the x-axis) at constant temperature. The graph is represented in the form of V=f(p) in which V is the amount of substance adsorbed and p is its partial pressure (or concentration) of the species to be adsorbed.

By varying the pressure and the temperature, the adsorbate (the species in the fluid phase) is either adsorbed or desorbed, until reaching the equilibrium with the surrounding environment. This leads to the fact that, by cyclically changing the environmental conditions, it is possible to adsorb one (or more) component of a mixture of gases, and thus increases the relative amount (in percentage) of the other components in the gas. This is the principle behind Pressure Swing Adsorption (PSA) and Temperature Swing Adsorption (TSA), that are systems commonly used to purify gases. The knowledge and the study of the isotherms are very important to structure the adsorption cycles to be as effective (and efficient) as possible. The first isotherm model has been developed by Irving Langmuir [28] connecting the adsorption of some gaseous species on surfaces. The first correlation at all between the amount of a compound in a liquid and in the gas over it was done by the already mentioned W. Henry at the end of the XVIII century [25].

The types of isotherm change dramatically according to the interactions between the materials involved; according to the desired output, it is necessary to carefully choose the coupling of materials. There are many studies about this topic, and from the shape of isotherms, it is possible to analyze the different behavior of the molecules and their properties. Figure 9 shows an example of isotherm, which is adsorption of CO_2 on different zeolites. It is interesting to notice how the shapes resemble each other, and each structure allows different quantities of adsorbate to be adsorbed on the solid; it is a consequence of the microscopic structure of the zeolites.

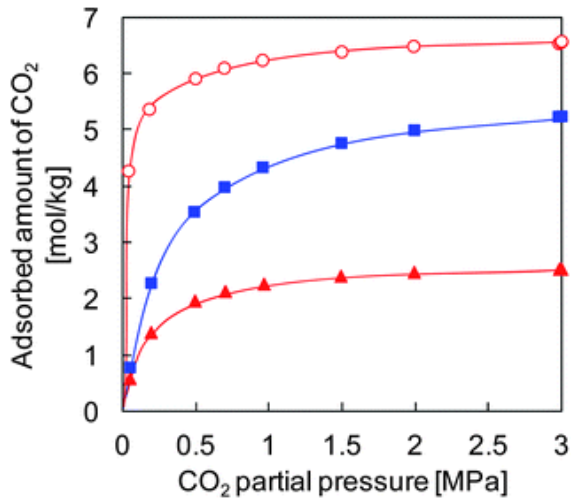

Figure 9. Examples of adsorption curves for CO2 on different types of zeolites: zeolite 13X (circles), Si-CHA (squares), Si-DDR (triangles). [29]

Isotherm diagrams are used, together with other applications, for the determination of the characteristics connected to the adsorbent's surface, such as the specific area and the pore size distribution. The specific area of the solid determines important characteristics such as the reactivity to substances, which is extremely important, for example, for the studies on catalysts. An important parameter that is used in this case is the monolayer capacity, which is the amount of adsorbate that can be fitted in a single layer on the adsorbent [30].

The types of isotherms that are usually observed in experimental data were categorized into 6 main types, whose shapes are in Figure 10 [19]. This categorization has been done thanks to the studies of Brunauer and others [31]. Starting from Isotherm I, it is shown that with increasing pressure the amount of gas adsorbed initially increases, often in an almost linear manner, but reaches a limit after this sharp increase at lower partial pressures. There can be two main cases where this type of behavior is observed: in the one case, there is actually a monolayer structure upon which a second layer can't be built; on the second case, there is extensive micropore condensation occurring and the saturation that occurs is not associated with the existence of a monolayer but rather with the filling of all the pores with condensed liquid.

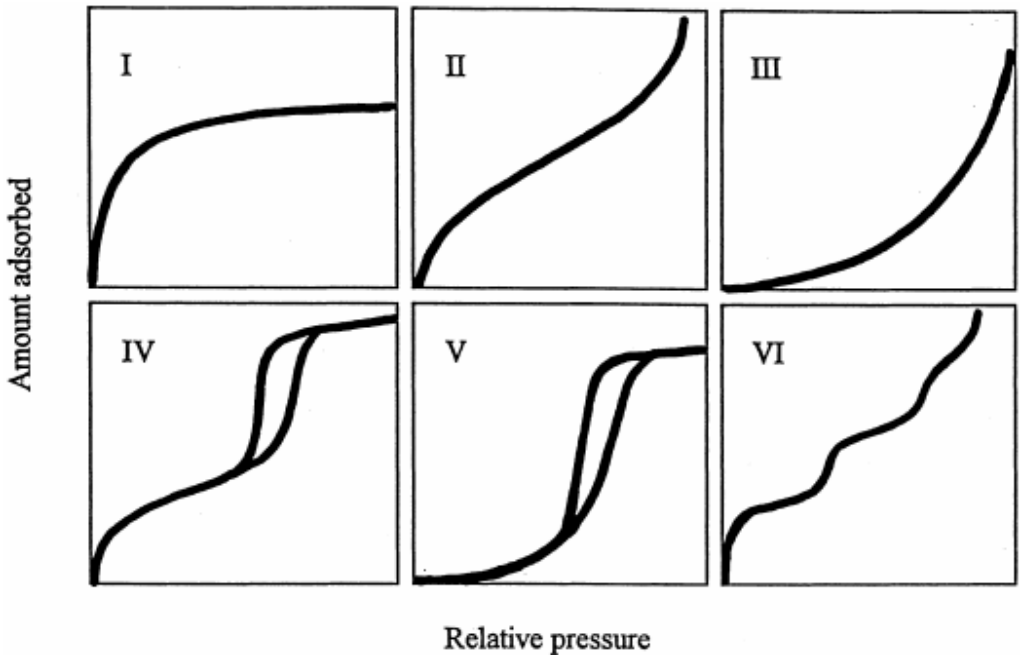

Figure 10. IUPAC categorization of isotherms [19]

Isotherms of type II shows the construction of multiple layers over the first one, as it is possible to notice from the region with a constant steepness in the middle of the graph; it is obtained both with a non-porous or a porous adsorbent. For multiple layers to occur the interaction between adsorbate molecules should be significant so that after the formation of the first monolayer more adsorbate molecules can adsorb on the already adsorbed adsorbate molecules. Isotherms of type III are quite rare and are related to the construction of multiple layers of adsorbate in which the heat of adsorption is less or equal to the heat of condensation. In this case, the interactions between sorbate and sorbent are low. These are related to type II isotherms in the sense that multiple layers do occur but imply a weak interaction between the adsorbate and the adsorbent.

Isotherms of types IV and V are characterized by hysteresis loops. Hysteresis occurs in many physical phenomena, and it is connected to the different states in adsorption and desorption phase. It is, in other words, the sign of the "past" of the phenomenon that is under study. In the case of adsorption isotherms, the forces involved in the adsorption and desorption phases are not exactly coincident (which means that they are not solely a function of the partial pressure) and the amount of gas adsorbed in the solid is not only dependent on the partial pressure in the analyzed situation but also on the state of the surface itself, in particular to the existence of pore condensation. Isotherms of type IV are typical of mesoporous industrial materials, and present a similar mechanism to the isotherms of type II, while type V isotherm is connected to the type III, and similarly to this latter, they are rare, as the adsorbent-adsorbate interaction is weak and there is no clear separation between the construction of a single layer or multiple layers. Isotherms of type V are connected to a small number of porous materials.

Isotherms of type VI present instead many different steps that represent the building of multiple layers of molecules on a uniform non-porous surface. The step height represents the monolayer capacity for each adsorbed layer since each step recalls the shape of type I.

2.5 Adsorption mechanisms

After having seen the different types of adsorption patterns from the macroscopic point of view, the analysis can be now focused on the mechanisms of adsorption on the microscopic level.

Monolayer adsorption occurs in two common cases that are chemical adsorption and physical adsorption on microporous materials, like activated carbon [22]. Chemical adsorption presents a monolayer behavior because of the chemical interactions between the adsorbent and the adsorbate molecules which only allow the formation of chemical bonds on a single layer of molecules; in the case of zeolite adsorption, for example, instead, there is a precise amount of adsorbate that can fit gradually within the pore space, as its partial pressure increases; since the pore radius is very small this implies that pore condensation occurs at very low pressures and saturates the material. This isotherm pattern is of type 1 in BET classification, and when the threshold is reached, adsorption of further molecules is basically stopped.

The porosity and the pore size are important parameters, as the ability to adsorb a substance is directly connected to the area of the material, together with the volume available in smaller pores. In general, the materials that are chosen for adsorption have an extremely wide effective specific area that may reach hundreds of square meters per gram of adsorbent (m^2/g). The structure of the materials can change deeply the kinetic and the type of isotherm. According to IUPAC, the pores of a material can be characterized according to the following groups [19]:

- Macropores: Pores with width > 50 nm
- Mesopores: Pores with width between 2 and 50 nm
- Micropores: Pores with width < 2nm

The possible occurrence of multiple layers is usually connected to physical adsorption and to micropore condensation. To better explain it, it is possible to imagine a situation in which a surface has been completely cleaned of the impurities and by the gases previously adsorbed on its surface. At the beginning, a small partial pressure of the adsorbate gas is applied, and its molecules will distribute on the surface far away from each other. Increasing the pressure, the new molecules deposited will form a uniform monolayer on all the surface. At this point the multilayer construction takes place. The first places to face this situation are the pores and the irregularities; going on with the pressure increase, the smaller pores will undergo a phenomenon known as capillary condensation, in which the adsorbate changes phase even if the partial pressure if well below the saturation vapor pressure [30]. Capillary condensation is described as "the process by which multilayer adsorption from the vapor phase into a porous medium proceeds to the point at which pore spaces become filled with condensed liquid from the vapor phase" [32]; Condensation occurs at partial pressures well below the saturation vapor pressure because of the van der Waals interactions, that are intensified because of the surrounding smaller volume.

The whole accessible volume present in micropores can be regarded as adsorption space and the consequent process is micropore filling by capillary condensation. Adsorption in micropores is defined as a primary physisorption process, which is different from the adsorption mechanisms that occur in mesopores and macropores. In mesopores, after multilayer adsorption, the residual volume is filled with condensate, separated by the gas by menisci [19]. This is because the pressure needed for condensation decreases sharply inside a small pore. This fact shows how condensation and adsorption can be close, and the influence that condensation heat has on adsorption heat in the physical adsorption.

When dealing with micropores, the preferred unit of measure is the Ångstrom (Å) that is equivalent to 10^{-10} m. The limits to pore filling mechanisms are quite arbitrary and depend on the type of material and, as a general statement, smaller molecules will diffuse better in comparison to bigger ones. Pore size has a significant bearing on the ability of a given solid to adsorb certain molecules, in particular in the case of molecules which are of sizes comparable to the pore diameters. In solids with very small pores, the diffusion of the adsorbate molecules through the pore structure may be hindered by their size, with larger molecules diffusing slowly through the pores. In this case, some molecules may be too big to be adsorbed in the solid and thus remain in the gaseous phase, and a molecular sieving effect will be observed. Molecular sieving is a common separation process, and the molecular sieves will be presented in the "Commonly used adsorbents" section.

It is worth to name the types of intermolecular forces that occur during physisorption [20]:

- Dispersion forces: they represent the most critical component. They are the effect of the rapid movement of the electron, which creates an oscillating dipole moment. This contribution is always present with all the types of adsorbents, while the other ones are present particularly with the zeolites, that present an ionic structure.
- Ion - dipole interaction. They are the interactions between a solid ion and a polar gaseous molecule.

- Ion - induced dipole interaction. They are the interaction between a solid ion and a polarizable gas molecule.
- Dipole - dipole interaction. Interactions between a polar solid and a polar gas and a polar gas molecule
- Quadruple interaction. They are represented by the interactions in symmetrical molecules, such as CO_2.

The characteristics of the surface change deeply the properties of the adsorption; in physical adsorption, is extremely important to define the surface structure (homogeneity, pores etc.) and the capability of the molecules to have translational, rotational and oscillatory movement [33].

Some of the main empirical models that can be named are [22]:

- Langmuir model
- Langmuir-Freundlich model
- BET theory

As can be imagined, each of these theories has an adequate range of applications and needs to be carefully chosen according to the experimental data connected to the materials chosen.

2.6 Adsorption models

The thermodynamic approach to adsorption equilibrium is general and has the same theoretical basis as the other types of chemical equilibria. The possible approaches are two: the surface of the adsorbate can be either considered as a single phase having the properties of a solution or, if the properties of the adsorbent are inert, the adsorbed molecules are regarded as a distinct phase [22]. This theory was developed by the American scientist J.W. Gibbs and allows to obtain more information in comparison to the former approach [21].

2.6.1 Linear model – Henry's law

From thermodynamic considerations, it can be assumed that, at sufficiently low concentration, the equilibrium isotherm will tend to linear. This fact is consequent to Henry's law, that states that the amount of gas dissolved in a liquid is proportional to the partial pressure of the gas in contact with the liquid [25]. Expressing it mathematically, it results in

$$\lim_{C \to 0} (\partial q / \partial C)_T = K \tag{5}$$

with *K* representing the thermodynamic equilibrium constant, dependent on the temperature by a van't Hoff equation:

$$K = K_0 e^{-\Delta H_0 / RT} \tag{6}$$

This dependence shows that the adsorption capacity increases with decreasing temperature.

The assumptions on which the application of Henry's theory is valid are that:

- There is no competition for adsorption sites

- There is no interaction between adsorbed molecules

Since these effects become important with increasing loading, the shape of the isotherm will be affected together with the heat of adsorption [34]. Even with the case of complex geometries, if the potential field around the geometry of the solid is known (particularly inside the micropores) the dimensionless Henry's constant can be calculated by integrating the function over the micropore volume. This fact is useful in predicting the behavior of zeolites and other materials that have a known geometry; it is instead not effective in the case of amorphous materials such as activated carbon.

Henry's law is equivalent to an ideal gas type of equation regarding the adsorbed layer.

2.6.2 Langmuir model

Langmuir theory is the simplest model to explain monolayer adsorption. The work was carried out by the American chemist Irving Langmuir, who was awarded in 1932 with the Nobel prize thanks to his contribution to surface chemistry.

The theory is based on some main assumptions made on the surface and in the way of bonding with the adsorbate. The symbols are the ones used in Ruthven's book [22].

- The adsorbent surface has a certain amount of adsorption sites q_s, which are partly occupied by adsorbate molecules q and partly vacant
- Each site can hold one adsorbate molecule
- All sites are energetically equivalent
- There is no interaction between molecules adsorbed on neighboring sites
- Adsorption – desorption is a process similar to condensation and evaporation
- The rate of condensation is proportional to the number of vacant sites while the evaporation is proportional to the number of occupied sites

Considering these assumptions, the mathematical section will be carried out in the next paragraphs. Two constants, k_a and k_d, are defined as connected to the number of sites and to the sorbate partial pressure p

- The rate of adsorption is defined as $k_a \cdot p \cdot (1-\vartheta)$
- The rate of desorption is defined as $k_d \cdot \vartheta$
- $\theta = q/q_{sat}$ is the fractional coverage

In equilibrium conditions, it is possible to state that:

$$\frac{\theta}{1+\theta} = \frac{k_a}{k_d} p = bp \tag{7}$$

In this equation, *b* is the adsorption equilibrium constant and is related to the temperature by the Van't Hoff equation:

$$b = b_0 \exp(\frac{-\Delta H0}{RT}) \tag{8}$$

The parameter *b* is fundamental to describe the behavior of an adsorbent. The two most important parameters that are specified to describe the adsorption curves are usually the b coefficient and the maximum amount of adsorbate that can be stood by the solid, q_{sat}. Rearranging the equation (7) keeping in mind that $\vartheta = q/q_{sat}$, it results that:

$$\theta = \frac{q}{q_{sat}} = \frac{bp}{1 + bp} \tag{9}$$

This formulation shows the asymptotic behavior of this adsorption profile, thus relating to the Isotherm of Type I; it results as well that $q/p = bq_s - bq$. When pressures are very low, it results in

$$\lim_{p \to 0} \frac{q}{p} = bq_s = K \tag{10}$$

This equation indicates how, at low pressures, Langmuir model follows closely Henry's law. A direct correlation at low pressures is shown in Figure 11, with the lines showing the theoretical plot and the dots showing the experimental results.

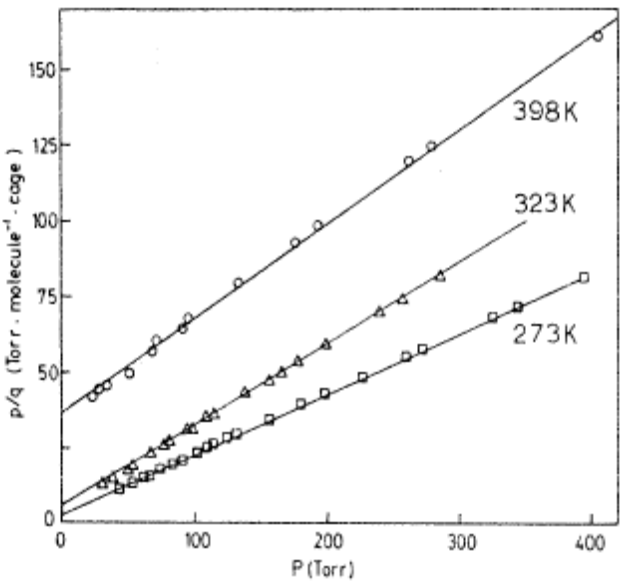

Figure 11. Langmuir plots showing conformity to Langmuir equation, on propane with 5A zeolite [22]

Langmuir shape of the equation fits well with the isotherms of type I, as it shows the same asymptotic behavior as the partial pressure tends to 0 and when it tends to high amounts of adsorbate. Figure 11 shows the conformity of experimental data on adsorption properties of zeolites to the Langmuir plot.

The limit of Langmuir's model is that it isn't quantitatively reliable as the loadings increase; there are many different models that try to explain the behavior of multilayer adsorption.

Langmuir's model can be derived from Gibbs formulation. The mathematical derivation it rather long and needs many mathematical steps; for a more detailed study, the extensive explanation can be found in Ruthven's "Principles of Adsorption" [22].

2.6.3 Freundlich model

Freundlich isotherm is a model describing the non-ideal and reversible adsorption, with the possibility of formation of multiple layers [35]. It demonstrated that the ratio of adsorbent over adsorbate was non-constant at different concentrations of sorbate [36].

This theory is used in heterogeneous systems in which there are organic compounds or highly interactive species on activated carbon and molecular sieves. The critics to it are the fact that it is lacking a fundamental thermodynamic approach and it is just empirical, not approaching Henry´s law at low pressures. Because of these reasons, it will not be further considered in this work.

2.6.4 BET theory (Brunauer – Emmet – Teller)

As previously stated, one of the fundamental parameters of an adsorber is its specific area and a major problem is to calculate it exactly [34]. The obvious way to calculate the area would be to have a complete monolayer and thus calculate the total area by knowing the amount of gas adsorbed. This might be possible in chemical adsorption, but in physisorption, the second and further layers start to form well before that there is a complete uniform first layer.

Brunauer, Emmet, and Teller developed a simple model isotherm to account for multilayer adsorption, and later on, calculate the monolayer capacity [37]. Although it is not as well completely accurate, it is still now the most commonly used method. The great problem arising when developing an exact method is the fact that the forces between sorbate-sorbate molecules are comparable to the sorbent-sorbate interactions. Thus it is important to mention the simplifications on which the BET model is based [22]:

- Each molecule on a layer provides a site for the subsequent layer
- The molecules in the second and subsequent layer behave as saturated liquid
- The equilibrium constant between the first layer and the subsequent layers is different

Langmuir and BET theories, when applied in a practical case, result in two different shapes of the adsorption curve. An example regarding the amount of shale gas adsorbed in rocks according to the two theories is reported in Figure 12.

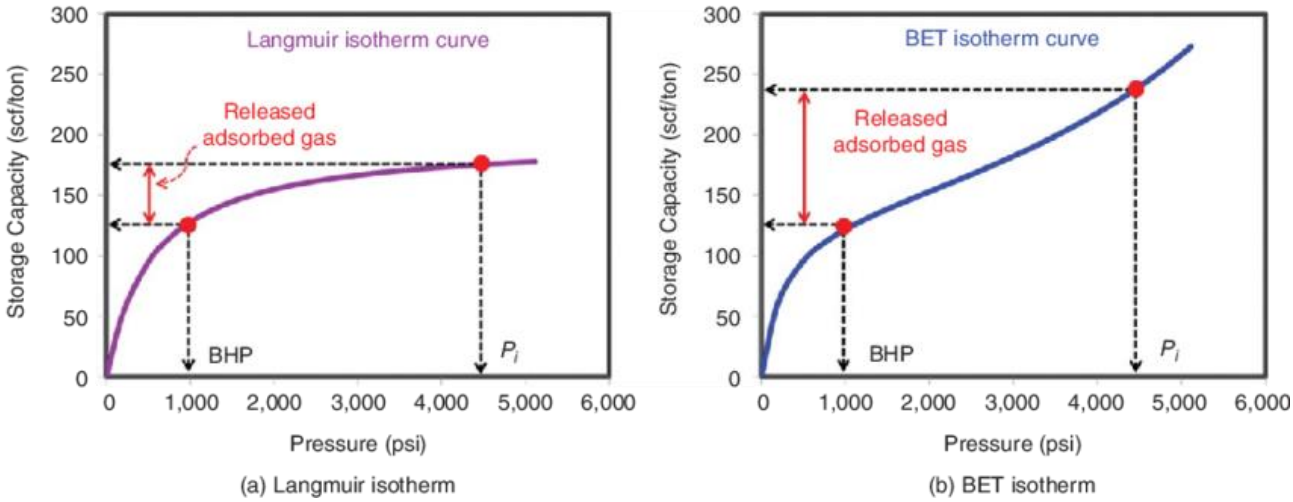

Figure 12. Comparison between the Langmuir and BET plot. The example was taken from the capacity of shale gas adsorption by rocks at high pressure during the desorption phase [38]

The resulting equation for BET model is:

$$\frac{q}{q_m} = \frac{b(p/p_s)}{(1-\frac{p}{p_s})(1-\frac{p}{p_s}+\frac{bp}{p_s})} \tag{11}$$

and represents the basic isotherm of type II. It has been found that it provides a satisfying representation of the experimental data with 0,05<p/p_s<0,3.

Using Langmuir or BET isotherm as the base to model a real system can lead to very different data when compared to Langmuir isotherms; to cite an example, in Figure 12 there is a plot showing the different quantities of gases that can be adsorbed in rocks at very high pressure in a shale gas deposit [38]. At the same pressure, the two approaches lead to results that are completely different; this is why there is a multitude of other isotherms considering two or three parameters. A comparison of them and a brief overview can be found in an article from Foo from 2009 [36]. BET theory is often used to estimate the specific surface of porous materials.

2.7 Linear driving force model

The Linear driving force model – or LDF model – is frequently used for the representation of adsorption columns and for the dynamic effects that adsorption has. It is a simple, analytic and physically consistent methods, and is represented by just a simple equation with few factors dependent on the current conditions of the point in analysis and the surrounding environmental conditions. It is not as rigorous as the Fickian diffusion model, but it has been demonstrated that the kinetics of the single pore is essentially lost once the whole bulk of the adsorbent is considered, and the adsorption model is applied on heterogeneous solids, or in the case of calculating the breakthrough curves [39].

The equation that describes the phenomenon is:

$$\frac{\partial q_i}{\partial t} = k_{ldf}(q_{sat} - q_i) \tag{12}$$

In which the term k_{ldf} indicates the linear driving force constant, concerning the velocity of the adsorption phenomenon in the solid. This constant is usually obtained in an experimental way, and it is practically important as its value is connected to the cycle time and the dimensions of the reactor.

2.8 Commonly used adsorbents and their applications

There are many possible types of adsorbents, with different adsorption curves and parameters. During practical processes, an important phenomenon is represented by the coupling of two (or more) different compounds that can change a lot and the performance of the process. There are three main types of adsorbents that need to be named:

- Silica gel
- Activated carbon
- Alumina
- Zeolites

This chapter will describe these materials, their characteristics, and their main applications.

2.8.1 Silica gel

Silica gel is a polymeric acid partially dehydrated, with the general form $SiO_2 \cdot nH_2O$. It is a granular and porous form of silicon dioxide, obtained from sodium silicate. It presents a microporous structure and a strong attraction to nonpolar molecules such as water. The polarity is given by the hydroxyl group present in the water molecule connected to SiO_2 that makes it have a great affinity to all polar molecules.

Its main uses are related to water, alcohols, phenols, and amines. A very common use of silica gel that is noticed in everyday life is its use as a desiccant, especially for the transport of electronic goods. Its usual appearance is in small spheres with the diameter of few millimeters, and transparent. Properties such as pore distribution and size depend on the different process used to manufacture it. Silica as a desiccant is a material presenting physisorption properties, as it can be regenerated by exposing it to high temperatures for a period of time.

Its adsorption isotherm presents a continuous increase in loading since multiple layers of adsorbate are added; silica gel in the case of commercial gels has an area between 350 and 750 m^2/g [40] that is a consequence of a very complex porous structure. Silica gel pores are not regular and present a various diameter distribution.

2.8.2 Activated carbon

Activated carbon is a material obtained by the thermal decomposition of carbonaceous materials and activated with the exposition to steam or carbon dioxide at elevated temperature. The structure is composed by microcrystals of graphite, united together to form a particle. The space between two crystals, that have different orientations, is the space that forms the micropores. The pore distribution and dimension are depending on the manufacturing process and the conditions of the pyrolysis. The process of activating the carbon at temperatures between 700 – 1000 °C is useful to remove the tars created during the pyrolysis and opening the pores [22].

Activated carbon is a material that does not have a repetitive structure. The distribution of pores is wide and is divided into the three categories of micropores, mesopores, and macropores. It also does not have a polar orientation, unless special treatments are performed; this makes it suitable for the adsorption of nonpolar molecules and can be used for example in water cleaning systems. Usually, the activated carbon used for liquid cleaning purposes has wider openings of the pores, in such a way to enhance the diffusion in it. It has as well different industrial applications in the field of gas purification, mining, and pharmaceuticals, to cite some.

Activated carbon can be as well manufactured with special activation procedures in such a way that the pore distribution is much smaller, ranging between 4 and 9 Å. The pore distribution is small, and the porosity is as well much smaller than in the normal case. In this configuration, the material is named "Carbon molecular sieve". Even if the process is clear, it is difficult to be able to reproduce it perfectly, so it is believed that the selectivity of a carbon sieve does not reach the selectivity of a zeolite sieve that has the size of the pores determined by its molecular structure.

2.8.3 Activated alumina

Activated alumina is a material manufactured from aluminum oxide. The surface is more polar than the alumina gel's and has both acid and basic behavior, because of the nature of alumina. It has a wide specific area (around 200 m^2/g) even though lower than activated carbon or zeolites.

It is used as a desiccant from water, and as a filter for polluting substances such as fluoride, arsenic or selenium in water. It is used as well as a catalyst in some industrial applications. Alumina is not as much used as in the past, as molecular sieve adsorbents have replaced many of its uses because of their higher capacity and a lower equilibrium vapor pressure.

2.8.4 Zeolites

Zeolites are porous crystalline materials. They are structured on a matrix of aluminum and silicon, thus the name aluminosilicates; their basic structure consists of a composition of SiO_4 and AlO_4 tetrahedra, joined together in various arrangements through shared oxygen atoms [22]. Their feature is to have a regular pattern of atoms that allows having a very regular dimension of the pores; this fact is crucial in the adsorption mechanisms. Their name comes from the Greek translation "boiling stone" as it was noticed that, when exposed to high temperatures, the zeolites emitted steam [41]: today we know that it is the desorption process.

The general formula of a zeolite may be written as $M_{x/m} \cdot Al_2Si_{2-x}O_4 \cdot nH_2O$, where [42] :

- The first term corresponds to the non-framework cations
- The second term represents the framework components, the basic structure of the zeolite
- The last term is the sorbed water

And x represents the ratio between aluminum and silicon.

Each aluminum atom in the structure introduces a negative charge, (recalling the fact that Al is a metal of the III group while Si is a semimetal from the IV) and this fact unbalances the charge of the overall structure. The negative charge thus generated needs to be balanced by a cation that is located within the zeolite porous structure in specific sites on the structure and plays a very important role in the determination of the properties of the zeolite, in particular, adsorption. In general, the more a zeolite is rich in aluminum, the more it has an affinity towards water and polar molecules; on the other hand, the structures very rich in Si such as silicalite are essentially hydrophobic and tend to adsorb non-polar molecules such as paraffin. It is useful to project the zeolite composition with a focus on the material to be adsorbed.

The parameter that determines the diffusion properties in the crystal is mainly the free diameter of the intracrystalline structure. The pore openings are strongly dependent on the type of structure of the zeolite. These micropores have sizes comparable to the diameters of molecules, which is crucial in determining the suitability for a molecule rather than another. These openings are made up by oxygen rings that have configurations ranging from 6 to 12 oxygen atoms. Examples of common zeolite structures are reported in Figure 13.

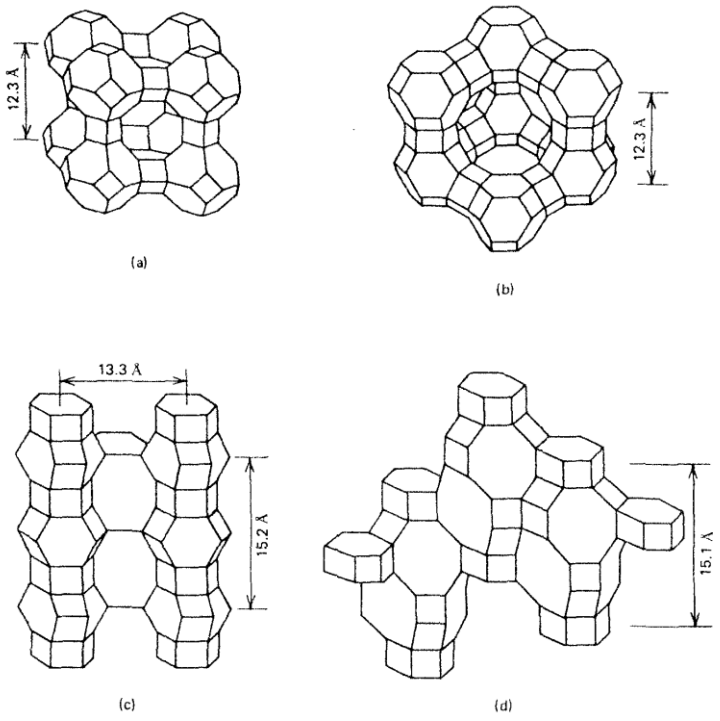

Figure 13. Various zeolite structures: zeolite A, zeolite X, and Y, erionite, and chabazite [22]

The structure of the zeolite crystals can be articulated into one, two, or three dimensions and has a regular pattern. It is useful to distinguish between the main types of zeolite used for adsorption purposes:

- Zeolite A: Its structure can be seen in figure 5. Its basic structure is composed of eight cages located at the corners of a central cube and connected by oxygen rings. Each cell contains 24 tetrahedral units, each one composed by AlO_2 or SiO_2. The x ratio (SI/Al) is close to 1.0 and there are 12 sites in which the cation can take place. The adsorption takes place in three steps: the first sites to be occupied are the internal edges followed by the spots close to the 8-oxygen rings (that are the entrances of the central

cube) and the last ones to be occupied are the external edges close to the 4-oxygen rings that connect the sodalites. During adsorption, a phenomenon that occurs is that the ions that have already taken place in the sites tend to block the entrance to the other incoming ions. This means that only smaller molecules can enter. An application for such a zeolite can be the drying of reactive hydrocarbons: the small diameter of the entrance does not allow the hydrocarbon molecule to enter the zeolite and purifies it.

- Zeolite X and Y: These zeolites present the structure represented in the image *b* in figure 5. They are composed by eight sodalite cages containing in total 192 tetrahedral units. The result is a very open structure, in which each cage is connected to four other cages; this means that relatively big molecules can penetrate this structure. The difference between X and Y cations is the different *x* ratio, which is higher in the case of Y structure. This turns out in the fact that the exchangeable cations that can be hosted on the Y zeolites are less than the ones hosted on the X (from 10-12 to 6 in the case of Y structure). In this case, the distribution of the cations is very complex and depends on the nature and number of cations.
- Mordenite: The special feature of this crystalline structure is the fact that its structure is unidimensional. This material behaves as a slow adsorber as even small molecules have difficulties in being adsorbed in it: the channels might be blocked by extraneous material. Because of this reason, mordenite is very sensitive to the presence of undesired molecules in the material under treatment.

In general, zeolites have a very broad application, because of all their different forms and molecular structures. Overall, in 2016 were known 232 different possible structures [43], having similar chemical composition. A study conducted in 2008 underlined the problems in understanding the behavior of the adsorbate molecules inside the zeolite, because of the difficulties in carrying out meaningful experiments; thus the need for simulations, that can help understanding both the correct use of adsorbents and the adsorbent – adsorbate bonds [44]. Zeolites are used in a vast number of industries, and their development and better understanding can bring big advantages in terms of process efficiency and feedstock saving. Zeolites can be found in nature, but in general in industrial applications, the zeolites are artificial, because of the purity required.

2.9 Outlook on fuel cells

A fuel cell is defined as “an electrochemical device that converts the chemical energy of a fuel directly into electricity by electrochemical reactions” [45]. The feature that characterizes the fuel cell in comparison to the other systems is that the chemical energy contained in the hydrogen fuel is directly converted into electric energy inside the cell, without the conversion efficiency typical of a thermal machine. In other words, a fuel cell is not limited by the Carnot efficiency, which is the highest efficiency that can be reached by a cycle, according to the laws of thermodynamics, and can reach up to 60%.

Fuel cells have attracted much attention in the last three decades because of their high conversion efficiency and because of their low emissions and low noise. Their structure is compact, in the meaning that power production does not require as much space as many other power installation, and can be tailored to fit in urban

environments, such as rooftops or basements. Together with this, there is an increasing interest in the wide commercialization of fuel cell in the automotive environment, thanks to its low emission and the fast refilling time, in comparison to battery electric vehicles. Moreover, a fuel cell has the advantage that it keeps working as long as fuel is supplied, and is not as limited by time like batteries.

2.9.1 Classification of fuel cells

The general scheme of the device is represented by an anode and a cathode, between which there is an electrolyte that allows the transmission of protons. The electrons are produced in the anode and recombined in the cathode while creating a difference of potential and thus Electromotive Force. Since a single fuel cell has a low voltage, for commercial applications the fuel cells are organized in stacks, in such a way to reach the desired power and voltage output. The stack is connected to a group of other control systems and devices that are useful to keep the operation going: this group of other devices is named “Balance of Plant” and is fundamental for commercial fuel cells.

The low emissions of fuel cells, as previously said, are a great advantage that makes them very interesting for a wide group of applications, from the automotive engine power supply to its use in portable devices such as cell phones or laptops. The reaction takes place, regarding most of the fuel cells, at relatively low temperature, and this fact allows to not emit nitrogen oxides. The reaction yields just water vapor and CO_2 (in different ratios depending on the type of fuel) without the emission of all the minor but toxic compounds that are present in the exhaust of engines.

Fuel cells are categorized according to some key features of their structure:

- The type of electrolyte: there are several types of electrolytes that have a wide range of working temperatures. In general, there is a tradeoff between sensitivity to pollutants and operating temperatures.
- The type of fuel: usually hydrogen or reformate, which is a gas rich in hydrogen derived from the reforming and the processing of hydrocarbons.
- The application: stationary or mobile generation

The most promising fuel cell type has been shown to be the Proton Exchange Membrane (PEMFC), because of its low operating temperature and more flexible applications: it is by far the main field of research for the automotive industry, and it is very interesting for the residential and small generation market as well; in fact, in the year 2015 ninety-five percent of the fuel cells sold in the world were of the PEM type [46].

The main limit to the wide use of fuel cell so far has been the fuel issue: hydrogen is by far the most commonly used fuel, but it has the problem of being highly flammable and difficult to store. Hydrogen is a very light gas that does not exist as a pure molecule in nature in its molecular form and needs to be artificially produced. The most common production systems are hydrolysis and hydrocarbon reforming, with the latest system widely used in the petrochemical industry. By principle, there is a wide variety of possible fuels to be used in fuel cells, but the engineering and technological limits have reduced them substantially to hydrogen and methanol alone.

The fuel cell that will be used for the application of this project is a PEM FC, running on syngas composed mainly of H_2 together with other minor impurities; because of this reason, this chapter will focus on this type of cell setting.

2.9.2 General structure of a fuel cell

The fuel cell has a fundamental structure based on an anode, on which the electrons are generated, a cathode, on which the electrons are absorbed, and an electrolyzer, which is the material through which the protons flow from the anode to the cathode. The design of a fuel cell is important to prevent technical issues, such as the membrane drying or short circuit, and many possible settings have been developed so far. A simple working scheme of a fuel cell is reported in Figure 14.

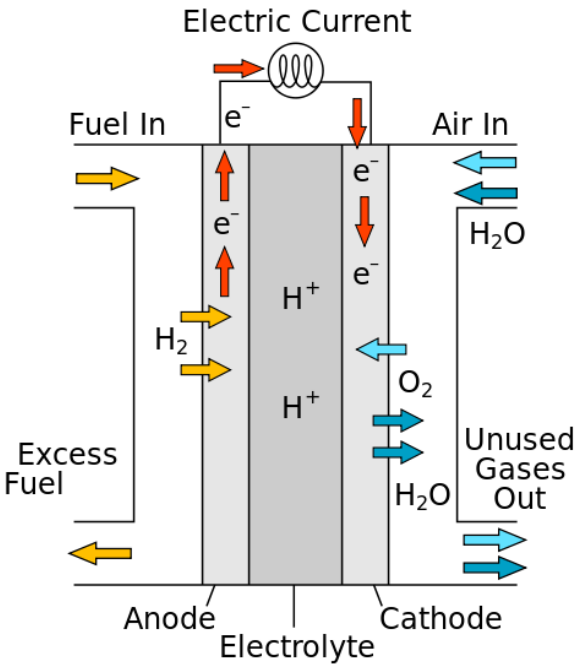

Figure 14. Schematic of a fuel cell running on H_2 [47]

The division of the reactants into single atoms is not easy, and it needs to be enhanced to make the reaction possible in a commercial device. There are three main ways of increasing the rate of the reaction:

- Increasing the temperature, shifting the equilibrium. Fuel cells have a very different range of operating temperatures, according to the type of electrolyzer.
- Increase the contact area between reactants.
- Use of a catalyst. Some catalysts allow to shift the equilibrium more towards the products; this is a fundamental point since the key deployment of fuel cells in the last years has been achieved with a better use of the precious catalyst, thus reducing the production costs.

The split of the feed molecules into single atoms occurs in the electrode, thus the electrodes are required to have all the characteristics just mentioned. The electrodes are produced with a material that allows having a very wide

contact area with the fuel; a commonly used electrode is activated carbon, which has contact areas of hundreds of times wider than the simple surface of the external shape. The design of this component and the fact that this part of the system contains reactants in three different phases (gaseous, liquid and solid) makes the planning of the electrode a vital part of the correct design of the fuel cell.

The flow of electrons from the anode to the cathode represents the useful effect of the reaction or the EMF. In the drawing presented in this review the system is represented as a single cell unit, in which the electrons flow directly inside the same cell; of course, many cells can be connected in series when the required power output is higher.

As previously mentioned, a single fuel cell can supply current at a low voltage - around 0.7 V during normal operations – which is not applicable to most of the practical applications. Fuel cell systems are usually composed of many cells connected in series forming a stack, in order to reach the desired potential difference output. The connection between the cathode and the anode of the next cell is thus extremely important: even if the voltage drop between the plates is small, if it is multiplied by each of the cells, can have a heavy impact on the total efficiency of the stack.

The solution is the bipolar plate: there is a component that connects the positive and negative electrode along their whole area, and at the same time supplies hydrogen to the anode and oxygen to the cathode. There are different characteristics that compete to each other in order to make a fuel cell working properly: in fact, the plate needs to be [48]

- A good conductor, to transfer electricity through the stack
- Do not allow leakages of the reactants before the electrodes
- Do not present a high flow resistance to the gas streams: in other words, having larger gas ducts, to minimize the pressure drop
- Be thin, to minimize the thickness of the fuel cell stack
- In many cases, having cooling channels, to remove the heat

To avoid the contamination of the reactants, the paths of the fuel and the path of the oxidant are perpendicular to each other; in this way, the manufacturing of the gas inlet is easier too. This component needs to be carefully sealed, as all the possible leakages of combustible gases are absolutely to be avoided, for safety and efficiency reasons. All these considerations make the bipolar plate a component of paramount importance for the proper working of a fuel cell.

2.9.3 Common fuels in fuel cells

The issue of the fuel is a key point in the definition of fuel cells. In principle, a wide variety of fuel can be used to power a fuel cell; from the practical side though, only hydrogen and methanol are actually used. The reason is the fact that to make the reaction happen, the fuel needs to be decomposed into ions, and performing this operation becomes more difficult with the increasing interatomic forces that are present in bigger molecules.

The hydrogen molecule is ideal from this point of view, as it supplies a high energy per unit mole, and the bond between the atoms is relatively weak in comparison, for example, to the energy needed to split the molecule of CH_4 (more than four times more) [49].

The use of different types of fuels is possible, but it needs to be taken into consideration that a part of the tension generated by the cell will be used to break the interatomic bonds, instead of being available as Electromotive Force. This phenomenon is present as well at the side of the cathode, in order to separate the hydrogen atoms; it is named, respectively, anodic overpotential and cathodic overpotential. The common alternative to hydrogen is methanol, while methane and carbon monoxide can be used as a fuel just by special types of fuel cells that work at very high temperature

2.9.4 PEM fuel cells

As previously mentioned, a type of fuel cell is the Proton Exchange Membrane fuel cell, shortly named "PEMFC". This type of fuel cell has the feature of using a special material as an electrode that conducts the ions (in this case protons H^+) from the anode to the cathode. This type of membrane has become extremely interesting from the commercial point of view because of

- Low operating temperature
- High power density
- Easy scale-up
- Fast start-up time

That makes it an ideal candidate for the small stationary and the automotive applications. In fact, according to recent market researches, the market share of PEM cells over the total of fuel cell units during the year 2015 was 95% [46]; during the next years the market value of the sector is supposed to grow by 26% annually as unit shipments and by 20% annually as the total power shipped [50].

The type of fuel cell on which the scope of this work is mainly about is the PEM fuel cell, because of the agreement signed between Cortus Energy and Powercell, a Swedish company that produces fuel cell with the purpose of using them in the automotive and stationary generation.

There are two types of PEM fuel cell that differ in their operating temperature: the low-temperature fuel cell works in a temperature range around 65-85°C, while the high-temperature type has a working range around 110-180°C. The advantage of this latter type over the former is the easier water and thermal management (since the temperature is over the evaporation point for water at atmospheric pressure) and the increased resistance to contaminants. The drawbacks, though, are a faster degradation and humidification issues on the cells.

The membrane that lays between the electrodes is made of particular materials that have a very high ionic conductivity, of which the most common is Nafion©, and at the same time prevent electron transport and the cross-over of hydrogen fuel and the O_2 oxidant [51]. They need to be chemically stable in an environment with the presence of radicals, mechanically robust and technically stable at the working temperatures of the fuel cell.

In the membrane space, two main transport phenomena take place: they are the ion transport and the water transport. The main driving force for the proton transport is the difference in potential, while the effect of diffusion in the material is relatively small.

The mechanism of ion transport is deeply related to the diffusion of water in membranes. It follows that, especially in PEM fuel cells, the humidification of the membranes is one of the main issues: to be conductive, a membrane must be humid, and at the same time, the electrodes can't be flooded with water. A system for the correct removal rate of liquid water needs to be implemented in almost all the PEM fuel cells, and a common solution is to use the fuel-air in order to overcome this function; the drawback from this solution is that a higher mass flow of air is needed, and thus a higher pressure drop is created in the plate.

Moreover, the system needs to be cooled, as waste heat is produced. The electrical efficiency of the cell is usually around 50%: according to the type of setting of the fuel cell, the heat generated in the reaction can be dispersed or used for other purposes; in the case of simultaneous heat and power production configuration (CHP), the system can reach a total efficiency of 85%. In general, all the fuel cells (except extremely small cases) present a cooling system, performed with the use of air or water that flows through the bipolar plate.

The overall reaction is:

$$2\,H_2 + O_2 \rightarrow 2\,H_2O \quad (\Delta H = 241.82\ kJ/mol) \tag{13}$$

Which means that, ideally, the only emission coming from a fuel cell is water. The partial reaction at the anode generates electrons, that flow in the electric circuit that connects the anode to the cathode and generate electricity; in the meantime, the H^+ ions flow through the membrane and react to form water in the cathode, together with the electrons and the O_2.

The purpose of research on fuel cells is to improve the effectiveness of their use, from the point of view of efficiency and from the point of view of production costs. The main issue in PEM fuel cells is the cost of the catalyst, which is in most cases a platinum-based material: the reduction of the amount of catalyst can deeply affect the final cost of the manufactured fuel cell. Thanks to the research of the last decades, the dramatic decrease of the amount of catalyst to be used on the electrodes has made fuel cell competitive with other generation technologies. In fact, the research on fuel cells has mainly focused on the reduction of the quantity of catalyst to be used on the anode and on the possible use of another type of material as a catalyst. The progress from the very first application of a fuel cell (in this specific case, an Alkaline fuel cell) has been very relevant: the first cells that served the Gemini missions had a platinum charging of 35 mg/cm2; the objectives for research for the year 2015 have been 0.2 mg/cm^2 and the 3M company has proved to achieve the charging of 0.15 mg/cm^2 with a PtCoMn alloy catalyst [52].

2.9.5 Fuel requirements for PEM fuel cells – International standards

The requirements from the fuel cell are a critical parameter that needs to be considered for the choice of the purification system. PEM fuel cells, because of the platinum-based catalyst, are very sensitive to carbon

monoxide, which can be considered the main issue regarding the purification of syngas produced from biomass gasification.

As a general figure, the amount of CO contained in the stream from biomass gasification ranges around 25% (molar), and if a Water-gas Shift reaction is applied this amount is reduced to 1-2%, according to the reaction conditions. A common way of industrially producing hydrogen is through methane (or other hydrocarbons) reforming, which involves a WGS reaction after it, reaches similar levels of CO.

Because of the sensibility of PEM fuel cells to contamination and poisoning from certain types of molecules, standards regarding the maximum amount of impurities have been set by international organizations such as ISO and SAE (Society of Automotive Engineers).

There are ISO specifications regarding the requirements for fuel cells both for the automotive and stationary uses; the former can be found in the ISO standard 14687-2:2012 in the "Part 2: PEM fuel cell applications for road vehicles", while the latter are in the ISO 14687-3:2014 under "Part 3: PEM fuel cell applications for stationary appliances". In both standards, the levels of CO and CO2 are 0.2 ppm and 2 ppm, respectively. The methane limit is in practice 100 ppm, as it is not considered as part of total hydrocarbons. In general, it is possible to state that stationary fuel cells can withstand a higher amount of impurities, as in this case higher Pt loading and Pt alloy catalysts can be used. SAE, from the USA, in the norm SAE J2719 suggests similar figures, with a further restriction on the amount of CO_2, set to 1 ppm.

The technical specifications on hydrogen such as grades are defined by CGA - G-5.3 – 2004 in "Commodity Specification for Hydrogen"

Table 2. ISO 14687-2 requirements for FCEV

Characteristic	**Type I, Type II**
	Grade D
Hydrogen fuel index (minimum mole fraction)	99,97%
Total non-hydrogen gases	300 μmol/mol
Water (H_2O)	5 μmol/mol
Total hydrocarbons *(Methane basis)*	2 μmol/mol
Oxygen (O_2)	5 μmol/mol
Helium (He)	300 μmol/mol
Total Nitrogen (N2) and Argon (Ar)	100 μmol/mol
Carbon dioxide (CO_2)	2 μmol/mol
Carbon monoxide (CO)	0,2 μmol/mol
Total sulfur compounds *(H2S basis)*	0,004 μmol/mol
Formaldehyde (HCHO)	0,01 μmol/mol
Formic acid (HCOOH)	0,2 μmol/mol
Ammonia (NH_3)	0,1 μmol/mol

Total halogenated compounds *(Halogenate ion basis)*	0,05 μmol/mol
Maximum particulates concentration	1 mg/kg

The European Union is developing a network of refueling points for hydrogen vehicles, in order to boost the use of this technology (especially regarding heavy transportation) (EU Directive 2014/94/EU). The fuel that is provided will comply with the standard ISO 14687-2.

The system will be prepared in order to later work in coupling with a fuel cell system manufactured by the Swedish firm Powercell, that has excellent performances with fuels that contain a high amount of undesired gases. Reaching the ISO standards limits with the syngas purification system would represent an excellent objective for Cortus, as it would open for the company the possibility of supplying the commercial network of hydrogen for automotive purposes.

3 Simulation of the system

3.1 Description of the setup

This chapter of the thesis contains a description of the setup that has been developed after the literature review and the system of equations describing the system.

Two possible solutions were selected: the membrane solution and the use of cryogenic distillation have been excluded, the first one because of the impossibility of reaching the desired purity, and the second because of the high cost for the compression of the gas and the connected inefficiency. The final system that has been selected for this task is the use of a PSA unit, possibly coupled with a water-gas shift reactor. Two different possible setups are possible for this aim and have been investigated in the simulations and a budget estimation, that will be presented in Chapter 5.3, has been prepared.

The first possibility that has been considered consists of a line in which the gas is treated through all the reactors and pure clean hydrogen is produced in order to power a fuel cell system. The second system differs in the fact that a recirculation system is applied: the stream of a PSA unit is always divided into two product streams, which are the product stream and the off-gas stream. The option that has been considered is to use the off-gas for a treatment into the WGS, in such a way that the yield of the reaction would be increased, by the fact of having more CO and less H_2 in the feed.

For this reason, the simulations have been performed with two different compositions: one group of simulations has been run with the measured percentages of the syngas at the outlet of the cleaning system, after the gasification reactor, while other simulations have been run with the hypothetic composition the syngas would have if a WGS would be performed on it. The gases are always considered as after condensation of the water formed, thus in the dry state.

The cycle that has been simulated is a Skarström cycle, with the PSA consisting of two parallel columns that work in an asynchronous way. The phases of the process are four, and are:

- Pressurization
- Adsorption
- Blowdown
- Purge

These phases are timed in such a way that the pressurization and the blowdown, and the adsorption and the purge happen at the same moment in the two different columns. This allows treating again a part of the gas coming from the adsorption into the column to be purged, in such a way that it is more effectively regenerated. A working scheme of the two-column setup is shown in Figure 15.

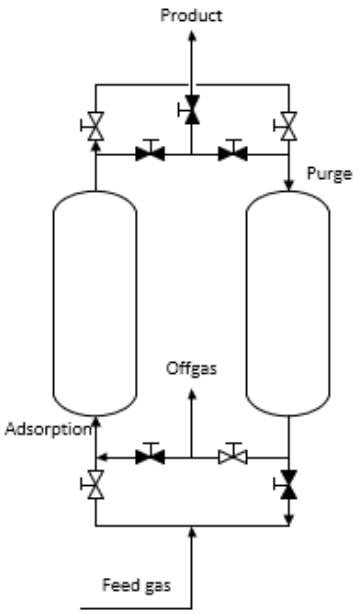

Figure 15. Scheme of the PSA that has been modeled. The black valves are closed; in this image, the left column is in adsorption phase and the right one is in purge phase

The simulations have been carried out for this work considering the flow rate at the outlet of the gas cleaning unit in Köping of 6 Nm^3/h, with the hope that the system will be implemented into a commercial unit in the coming future.

3.1.1 Scheme with a WGS and a PSA

This scheme allows all the stream to be subsequently treated in all the reactors: it is the setup that is mostly used by the steam reforming systems such as industrial plants and refineries.

The process can be divided into four main blocks, representing the steps of the chemical transformation:

1. The compression
2. The water-gas shift
3. The PSA
4. The fuel cell block

The feed gas is first compressed to high pressure; this value has to take into consideration all the pressure drops due to valves and equipment, and the required inlet pressure by the PSA unit. Originally, the possibility to use the steam already produced in the plant – at the level of 7 bar - was taken into consideration, but the fact that the flow rates are so limited poses a serious technical issue to this; it has thus been decided that the pressure will be set only as a function of the requirements of the PSA. It has been chosen to set the working pressures of the PSA to 14 bar as maximum pressure, and 0,2 bar as the lower. It has been attempted to use the ambient pressure as desorption pressure in order to save energy for the vacuum pump, but the desorption was proven

to be too slow. The system is planned not to need of a further recompression, to avoid costs and possible malfunctions.

As it has been described during the literature review, the stream is treated through a water-gas shift reactor that converts most of the carbon monoxide into carbon dioxide, less toxic for the fuel cell system, and at the same time increases the amount of hydrogen. The result of this first reaction is that the molar flow of gas is increased by about 60%, and the concentration of carbon monoxide drops from about 25% to around 1% [53]. The gas is later cooled down to ambient temperature, in such a way that all the water vapor contained in the stream condenses, and is prepared to be treated through the Pressure Swing Adsorption unit. In Figure 16 it is reported the process flow diagram of the solution; this drawing shows only the main reactors without taking into consideration the control system and the instruments.

Figure 16. Process flow diagram of the direct system

Between the main reactors, there are buffer tanks (not shown in the process flow diagram) in such a way that the flow is not strictly dependent on a particular unit. In fact, a limiting issue that has been faced during the research for the possible supplier is the fact that PSA systems are usually treating big flowrate of gas: PSA are usually designed for industrial capacities of thousands of cubic meters per hour of product. A way to solve this issue is to use vessels between the units, in order to work in batch mode and not with a continuous process.

The stream is treated in the PSA unit according to the calculations that will be shown on the following pages; the calculations have been implemented on a single bed, while in the reality these units have usually multiple beds linked by non-synchronous phases, in a custom-optimized way. As an approximation of a real system, it has been chosen to use a configuration with two beds connected to each other, in such a way that the purging of one bed is done with a part of the purified gas coming from the other bed, that, at that time, is working on the opposite phase.

The complete P&ID (Piping and Instrumentation Design) is shown in the Annex; in that version, all the auxiliary and complementary systems are shown.

3.1.2 Configuration with a PSA and a final blending

An alternative scheme has been developed as a possible variation to the previous setup, and consists of a double stage of PSA, with the treatment of the off-gas of a first PSA in a reaction branch in which there is a second PSA. The off-gas stream is recompressed once it exits the first PSA unit; a process flow diagram is reported in Figure 17. This system allows a more flexible control of the gas composition, foreseeing other possible uses of the produced gas that in such a way could be more suitable for the use in combustion engines. For the current application, the side stream will consist of a higher percentage of CO, thus allowing the water-gas shift reaction to be more effective thanks to the enhanced kinetics, and have a higher conversion into the useful H_2 product.

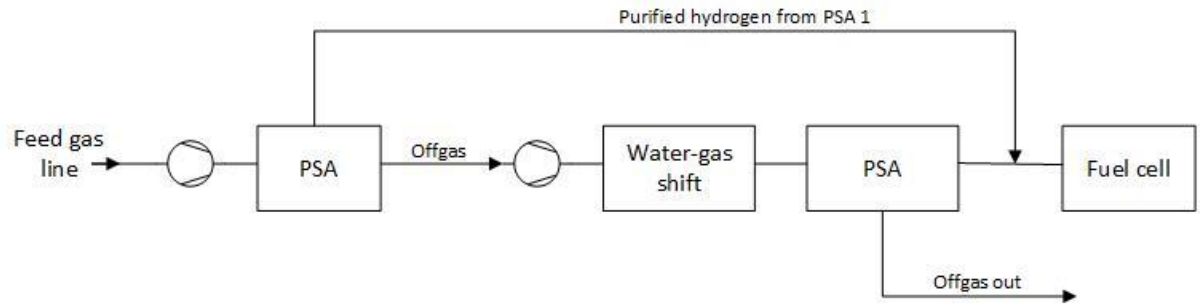

Figure 17. Process flow diagram of the system. Notice the compression of the off-gas from the first PSA

The setup is similar to the configuration previously presented, but slightly more complicated: there is an additional block of PSA and an additional compressor for the pressurization of the off-gas coming from the first PSA unit. The system is composed thus of:

1. Compression 1
2. PSA 1
3. Compression 2
4. Water-gas shift
5. PSA 2
6. Fuel cell

The gas is brought to high pressure in a first compression unit and is treated in a first PSA. The refined stream is connected to a gas cylinder located before the fuel cell system, while the off-gas undergoes further recompression. After this stage, it is treated in a water-gas shift and a PSA; the refined stream is later connected to the gas cylinder located before the fuel cells.

The limiting issue of this configuration is the higher capital cost for the two stages of compression and, especially, the two PSA. These units have a high capital cost and face the problem of the small size of the unit, previously mentioned before: the second PSA needs to be engineered in such a way that treats a flowrate even lower than the first PSA.

The two PSA configurations will be considered in the simulations, taking into account the raw gas composition and the composition after a shift reaction; the assessment of a cost-benefit analysis is beyond the objectives of this thesis, and it can be considered for a future work.

3.2 Description of the simulation

The simulations have been performed in Microsoft Excel, relying on numerical methods. The set of equations that are used to describe the system have been reported in the literature for similar studies and for related topics [54].

To make a realistic model of the system, the reactor, that is supposed to be a column, has been divided into 5 slabs. Each slab is treated as a volume with uniform characteristics and parameters, on which the conservation

of mass and the equations describing adsorption are applied. The principle is that the mass flow can be modeled in such a way:

[accumulation] = [in] - [out] + [generation] - [consumption]

The radial effects are neglected in the whole column.

The equation relative to the particular case treated in this work, which is adsorption, is defined as the component mass balance on the slab:

$$\frac{\partial C_i}{\partial t} + \frac{1-\varepsilon}{\varepsilon}\rho_s \frac{\partial q_i}{\partial t} + \frac{\partial (uC)}{\partial z} = 0 \tag{14}$$

In this equation, C is the concentration of the component in the gas phase, ε is the porosity the adsorbent material and ρ_s is its density of the adsorbent, q_i is the amount of the component adsorbed in the solid. The mass conservation for the single slab reflects on the total reactor as the conservation of mass between the inlet and the outlet.

The term $\frac{\partial q_i}{\partial t}$ defined as the amount of adsorbed gas in the solid adsorbent, is described by the equation

$$\frac{\partial q_i}{\partial t} = k_{ldf}(q_{sat} - q_i) \tag{15}$$

In which the term k_{ldf} indicates the linear driving force constant, as it has been explained in Chapter 2.7; q_{sat} is the maximum amount of that substance that can be adsorbed in the solid, under the current conditions of temperature and pressure.

The amount of adsorbate at the equilibrium is a function of the temperature and pressure that the adsorbate has; for the current case, it is calculated with the equation previously mentioned in Chapter 2, with Equation 9 in the description of Langmuir's model. The equation is only dependent on pressure:

$$q_{sat} = \frac{q_{max,i} bp}{1 + bp} \tag{16}$$

q_{max} defines the maximum amount of adsorbate that can be loaded on the adsorbent, while b is a parameter that can be extrapolated from the Langmuir isotherm fitting, and p is the partial pressure of the gas component. The two parameters describing the function are named Langmuir parameters.

The adsorption phenomenon is influenced by the value of the Reynolds number, a parameter that describes the condition of the motion of the fluid according to the operating conditions. The Reynolds number inside a reactor is described by

$$Re = \frac{\rho_g \varepsilon u d_p}{\mu} \tag{17}$$

In which the conditions inside the reactor are considered: ρ_g stands for the density of the gas, u is the absolute velocity, d_p is the diameter of the adsorbent particle, and μ is the dynamic viscosity of the fluid. There is a range

of optimal values for adsorption in Pressure Swing Adsorption and it has been defined to be between 9 and 18 [55].

The gas has been treated as an ideal gas, following the general equation of perfect gases

$$pV = nRT \tag{18}$$

There are a few parameters that have not been considered in the model, mainly because of limits of the software and because, on the other side, their application would go beyond the objectives of this work.

The main effect that has not been considered is the influence of the temperature on the adsorption cycle. As previously mentioned during Chapter 2, the thermal effects in adsorption cycles can be relevant, especially in the case of a strong heat release once a molecule is adsorbed on the solid matrix. The capability of adsorbing a gaseous molecule decreases with the increasing temperature (and vice versa) and this is affecting the adsorption cycle in a negative way. The thermal effects have been neglected assuming the concentration of adsorbate sufficiently low so that the heat released by adsorption is carried away by the gas flow.

The pressure drops of the column, the valves, and the fittings have been neglected. This fact is not exact, but the pressure drop on the column has been calculated by using Ergun's equation, that relates the pressure drop with the velocity of the flow and the characteristics of the column, and the resulting pressure drop was small enough (measured in few tens of Pascal) that the whole effect of the pressure drops on the system has not been considered. The mass axial dispersion coefficient has been neglected as well. The simplification of the geometry is illustrated in Figure 18.

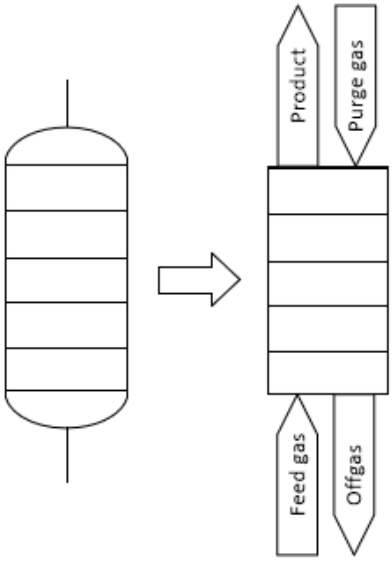

Figure 18. Representation of the modelized adsorption column

To solve the system of partial differential equations (PDE), that describe the pattern of the parameters according to space and time, discretization has been applied. The column reactor has been divided into 5 slabs with the same characteristics; the time is divided into steps of 1 second. The exact shape of the adsorption column has

been assumed to be a simple cylinder. The shape of the gas inlet itself is as well not considered, and the gas is supposed to flow uniformly through the whole section of every slab for each moment considered.

The system has been solved numerically with the forward Euler method, which is a first-order numerical method that is effective to solve systems of Ordinary Differential Equations (ODE). There are as well other methods to solve systems of ODE, but since the time step chosen is relatively short, this method has been judged as adequate.

The expression that describes Euler method is using the derivative of the function at the point considered and is calculating the value of the function in the next step by adding the product of the derivative and the time step to the previous value of the function. As an expression:

$$y_{n+1} = y_n + hf(t_n, y_n) \tag{19}$$

In which y_n is the value of the function at the point considered, and y_{n+1} is the value of the function in the next point.

3.3 Composition of the feed gas

3.3.1 Raw gas

The treatment of the raw gas produced by the WoordRoll process could occur in the case of a configuration with a double-stage PSA and a final blending before the fuel cell block. The pollutants such as ammonia and sulfur compounds, even if present consist an extremely small amount of the molar composition at the outlet (under the ppm) and have thus been neglected. The composition of the raw syngas is, as previously said, strictly dependent on the type of biomass used in the process; an average composition, assuming a general fuel as a feedstock, is reported in Table 3 [53]:

Table 3. Composition of the dry syngas not treated [53]

Component	% molar
H_2	59.1
CO_2	11.0
CO	27.9
CH_4	2.0

3.3.2 Gas treated with the water-gas shift reaction

The previous treatment of the syngas with a water-gas shift reaction enables to decrease substantially the amount of CO present if the product gas, and to make the cleaning of the gas before the fuel cell unit easier: compared to the composition of the raw dry gas, after the water-gas shift reaction the amount of CO is reduced by about 95% and the amount of hydrogen is increased by 10% [53]. At the same time, the total mass flow is increased thanks to the injection of steam.

Using the previous work of a colleague that has run simulations with heat and mass balances on the plant for a water-gas shift reactor, the following composition of the dry treated gas is assumed, as given in Table 4:

Table 4. Composition of the dry syngas, after the shift reaction **[53]**

Component	% molar
H_2	67.7
CO_2	29.8
CO	0.9
CH_4	1.6

As it can be noticed, the greatest change is in the relative quantities of CO and CO_2, with the latter increasing significantly. Most of the carbon is now contained in carbon dioxide: this fact makes the whole system safer as well since the carbon monoxide is a toxic compound and its leakage affects severely the health of the workers.

These figures are similar to the overall values that are reported for similar solutions of water-gas shift applied to the reformed gas from natural gas processing, in the case of industrial hydrogen generation [9].

3.4 Adsorbent materials

Two different materials commonly used for PSA units have been chosen as examples to run the simulations. The major limit faced in this work is that usually the adsorbent blend is chosen exactly for the separation of the syngas different molecules (in this case four) and often it is composed of different types of materials that are used together, in such a way that each type of adsorbent better adsorbs one type of molecule.

Moreover, the mutual interactions that exist between one molecule and another have an impact on the model of the system.

The two materials that will be simulated are:

- An Activated carbon, produced by Norit (The Netherlands), showing an amorphous structure [56]. Specific name: AC Norit R1 Extra
- A Carbon Molecular Sieve, produced by Carbotech (Germany) [57]. Specific name: Carbotech CMS H2 55/2.

This choice has been made according to the fact that these materials are a common choice for the composition of PSA adsorbents, and can represent well the general setup of the system; this analysis is also useful in the meaning of assessing if these materials are adequate for the required level of separation purity.

The Activated Carbon has been tested in a very similar setup [56] in order to produce hydrogen from a mixture of hydrogen, carbon monoxide, carbon dioxide and nitrogen; the values of the isotherms have been calculated according to experimental results, using a multicomponent adsorption gravimetric measuring system and are reinforced by theoretical values. The adsorption isotherms of this material can be seen in Figure 19.

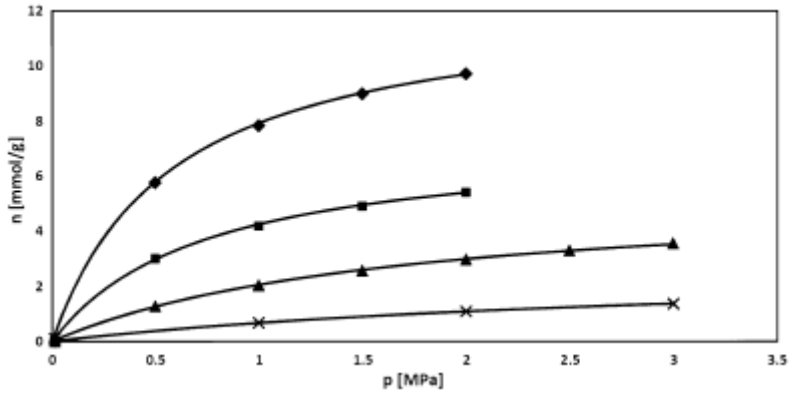

Figure 19. Langmuir adsorption isotherms on the Activated Carbon, Pure gas isotherms of CO_2 (black diamond), CH_4 (black square), N_2 (black triangle) and H_2 (times) [56]

The values of the Langmuir constants were calculated in the paper by Rother and Fieback [56] and are reported in Table 5 as follows:

Table 5. Langmuir parameters for the Norit R1 Extra

Molecule	n_{max} (mmol/g_{ads})	b (1/Pa)
CO_2	12.5	1.74
CH_4	7.41	1.35
H_2	2.87	0.31
CO	5.76	1.74
N_2	5.49	0.6

The value of the carbon monoxide adsorption parameters was not reported, as it was not present in the composition of the test gas considered in the abovementioned study. Its value has been estimated by observing the behavior CO and CO_2 have in the case of the Carbon Molecular Sieve, and translating it into the data for the Activated Carbon by making a proportion between the maximum amounts of CO_2 adsorbable in the two cases.

The value of the density has been estimated to be 450 kg/m^3 by checking the data of suppliers [58] and the data from other articles [54]; the porosity has been supposed to be 0.3 according to the same assumptions.

The Carbon Molecular Sieve has been selected after contacting one of the main manufacturers of adsorption materials, CarboTech, and asking for a material that could suit the specifics of the syngas produced by the WoodRoll® process to be purified. This same supplier had been selected for an experiment made by Kim and Young for the separation of CH_4 and CO_2 [54]; its parameters are reported in Figure 20.

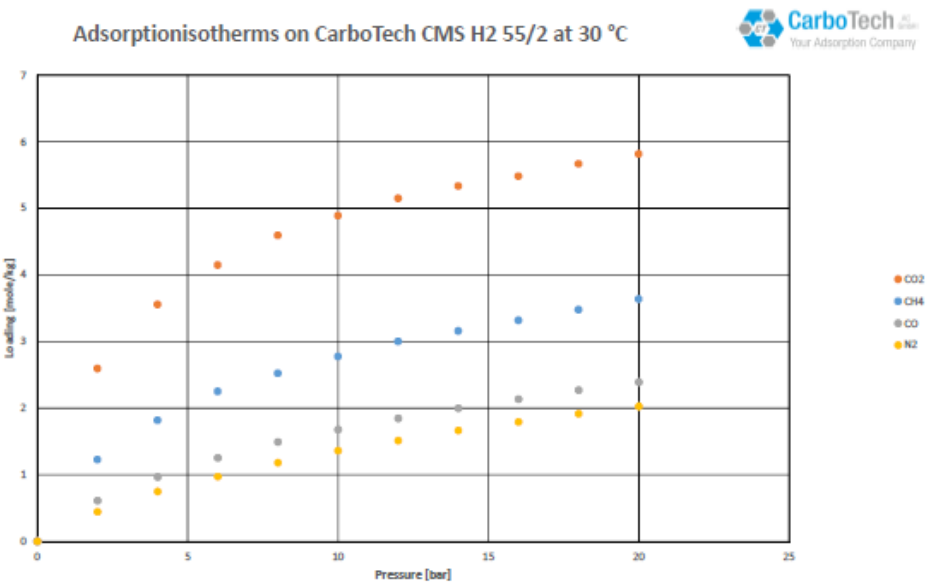

Figure 20. Carbotech CMS H2 55/2 isotherms for CO_2, CH_4, CO and N_2 [57]

The Langmuir isotherms values for the adsorption on Carbotech CMS H2 55/2 have been calculated according to the data contained in the information brochure. These values are as follows:

Table 6. Langmuir parameters for the Carbotech CMS H2 55/2 [57]

Molecule	n_{max} (mmol/g_{ads})	b (1/Pa)
CO_2	6.5	0.4
CH_4	4	0.4
H_2	0.5	0.6
CO	3	0.6
N_2	2.5	0.6

The issue of missing data applies in this case for the adsorption of hydrogen: it was not indicated in the brochure from the manufacturer, and its value has been estimated according to its behavior in relation to the fact that the molecular sieve technology allows to practically not adsorb a small molecule such as hydrogen, once it is especially prepared for this task.

In the information sheet, it was also specified that the bulk density of this material is 550 kg/m^3; the value of the porosity has been estimated to be 0.3 as similar to values found in the literature [54].

3.5 Variation of the system setup

The simulations have been performed in Microsoft Excel using the set of equations described in Chapter 3.2, and applying the forward Euler method in order to discretize the PDE. An assessment of the system has been done by varying the setup of the system with:

- The two types of feed-gas that the PSA are planned to receive
- The adsorbents
- The Reynolds number used in the adsorption phase

The thermal effects have not been considered, as has previously been explained. Although this could be a limit, the isotherms that have been found for both the materials were reported around 300 K; since this temperature is realistic after the syngas cleaning unit, it has been chosen as the constant temperature at which the simulation will take place.

The viscosity of the gases has thus been calculated at that temperature: the values for the chosen gases are reported in the table below. This figure is important for the calculation of the Reynolds number, dependent on a series of parameters between which the viscosity of the gas; the data used can be found in Table 7.

Table 7. Dynamic viscosity of the gas' components

Component	Dynamic viscosity [Pa*s]
H2	8.94E-06
CO_2	1.50E-05
CO	1.57E-05
CH_4	1.12E-05

The pressure is swinging between the values of 20 kPa and 1400 kPa, that are likely for this type of application.

The adsorption column is supposed to be a perfect cylinder with the dimensions of 1,5 meters of length and 0,20 or 0,25 meters of diameter, respectively in the case with a fast cycle and a slow cycle. The different Reynolds numbers have an influence on the amount of adsorbent that can be treated during the phase of adsorption: thus, for a slower flow, there is the need of having a wider diameter. The shape of the adsorption curve is strongly influenced by the kinetic parameters of the reaction, such as the LDF. This coefficient is important in order to set the adsorption times and the different phases of the cycle. In fact, a gas with a higher LDF coefficient will have a much faster adsorption, and the adsorbent will reach the saturation limit earlier. On the other hand, a gas with a lower LDF coefficient will be adsorbed in a much longer time, and a bigger reactor will be needed to purify the stream of gas.

These kinetic parameters were hypothesized according to the study made by Kim and Young [54]; the limit to this assumption is that it should be correlated with an experimental setup in such a way that time-related parameters such as the breakthrough curve could be measured, and from this data calculate the LDF coefficient.

The values chosen for all the cases analyzed were as follows in Table 8:

Table 8. LDF coefficients of the single molecules

Component	LDF coefficient
H2	0.005
CO_2	0.03
CO	0.019
CH_4	0.005

The values for CO_2 and CH_4 are taken from the article by Kim and Young [54], while the values for H_2 and CO are hypothesized, respectively, according to a slow adsorption in the solid and the ratio of molar mass with carbon dioxide.

The adsorption times are set to be equal in the pressurization and blowdown phase, and equal in the adsorption and purge phase. The case of short cycle has a total cycle time of 240 seconds, divided into 20 seconds for pressurization and blowdown, and 100 seconds for adsorption and purge.

On the other hand, the long cycle is 1200 seconds long and has a pressurization and blowdown time of 100 seconds, and adsorption and purge times of 500 seconds.

4 Results

The system has been tested for the condition present in the test plant of Köping, in which there is a 6 Nm^3/h stream of syngas that can be used to produce pure hydrogen.

The simulations have been carried out by changing the following three parameters:

- The adsorption time: the system has been optimized for a Reynolds of 9 and a slow cycle or a Reynolds of 18 and a quick cycle. The total cycle time was set to be 1200 seconds in the case of a slow cycle or 240 seconds in the case of the fast cycle.
- The adsorbent material: Carbon molecular sieve or Activated carbon
- The quality of the gas treated: the gas composition was considered as before the WGS or as after it

The simulations are stopped once the steady state is reached: this is defined as the condition for which the results of a cycle do not differ for more than 0,1% from the ones of the previous cycle if performed with the same conditions. The use of 1% of change is more often found in the literature [54], but since the outlet purity has slight changes between the cycles, it has been chosen to apply the difference of 0,1% for a better accuracy.

4.1 Setup of the simulations

The system has been plotted by using the calculations software Microsoft Excel, and the results have been plotted by using the built-in function. This section will introduce how the results were calculated and validated in the software.

As has been previously mentioned, two important parameters to take into consideration are the concentration of the gas in the different slabs (mol/cm^3) and the amount of gas that is adsorbed on the solid surface of the adsorbent ($mmol/g_{ads}$).

The following figures are showing the results for the case of raw gas, treated in a long cycle and with Activated Carbon as an adsorbent. The choice of this setup as an example was made as the graphs were clearest, but similar patterns can be found in all the eight simulations.

The effect of the adsorption parameters is clearly visible by plotting the graphs of the adsorbed amount of gas in the different slabs over time. In Figure 21 and Figure 22 are reported the patterns of the first four cycles (that can be identified by the rising or decreasing values). The first graph, indicating “bottom slab”, is showing the amount of adsorbed gas in the first slab from the bottom, thus the part of adsorbent that is first treating the feed gas. The behavior of thse top and bottom slabs are different, thus both of them are shown.

It is noticeable how the CO_2 is the most adsorbed gas in the bottom slab and its change of adsorption in the reactor is quite quick; on the other hand, hydrogen is only very slightly adsorbed, even though it has a partial pressure way higher than the other components of the gas mixture. It can be also seen that the adsorbent is not fully regenerated in the desorption cycle as the adsorbed concentrations of both CO and CO_2 remain high, which indicates that a longer purge time could be considered.

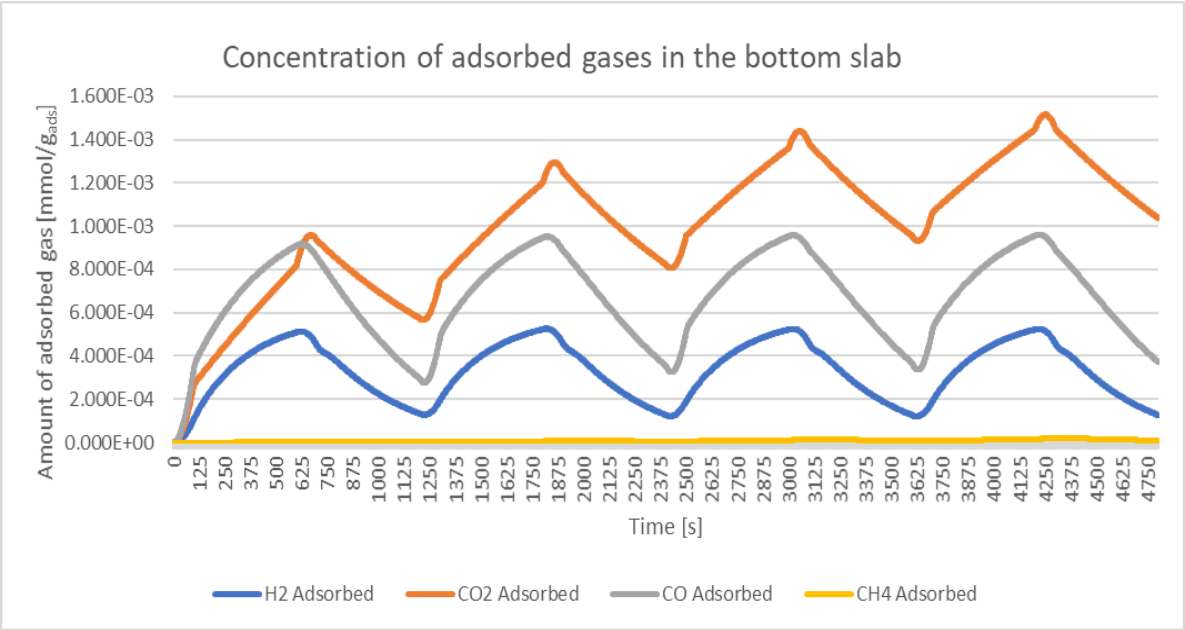

Figure 21. Adsorbed gases on the first slab of the adsorption column

Comparing Figure 21 and Figure 22, it can be noticed that the shape of the curves is very different, and it is as well the amount of gas adsorbed. While the first slab is quickly charged with CO and CO_2, the last slab is mainly charged with hydrogen. This is because the carbon dioxide is effectively removed in the reactor, thus almost no CO_2 arrives until the final slab; the gases that arrive are hydrogen and carbon monoxide, quantitatively more and also less adsorbed by the Activated Carbon. The curves present higher derivatives since the top slab is the first slab to receive the purging gas.

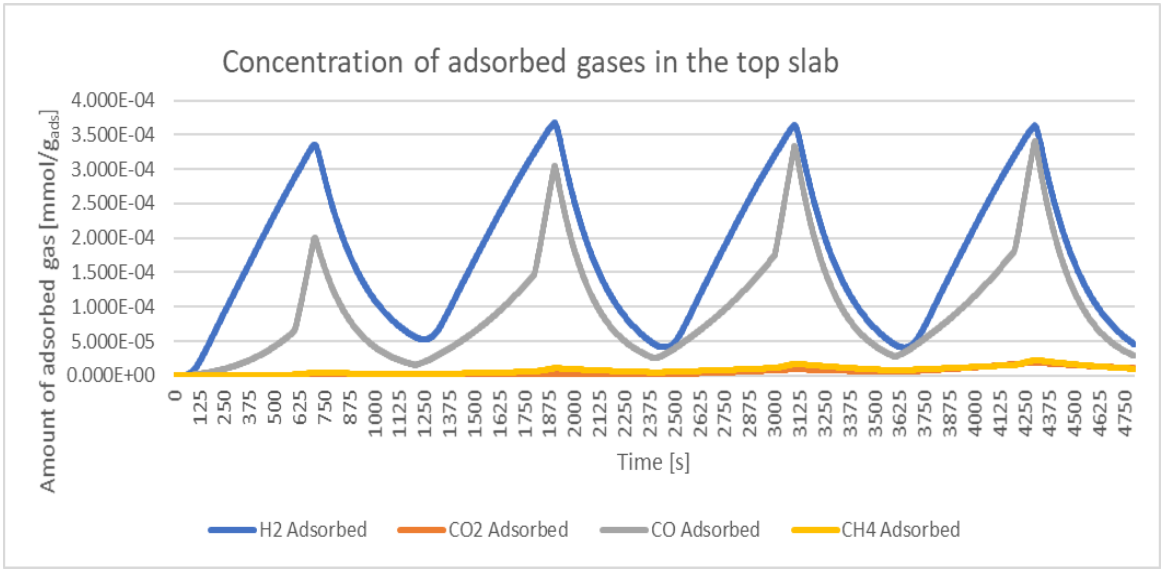

Figure 22. Amount of adsorbed gases on the top slab of the adsorption column

This configuration uses the counter-current flow, that allows having a better use of the adsorbent, in such a way that the amount of gas that can be treated with the same amount of adsorbent is optimized. The cost of the adsorbent, although not relevant for such as small application can become important in the case of big units.

In Figure 23 and Figure 24 are reported, as an example, the percentages of the gases at the outlet of the adsorption phase and at the purge phase. The gas at the end of the adsorption phase is later partly used as a product, and partly to regenerate the other column (which is in the purge phase). To simplify the model, the composition of the purge gas between the adsorption phase of a cycle and the purging gas of the same cycle is assumed to be constant, as if there was a vessel in which the product gas is stored and connected to the other adsorption column.

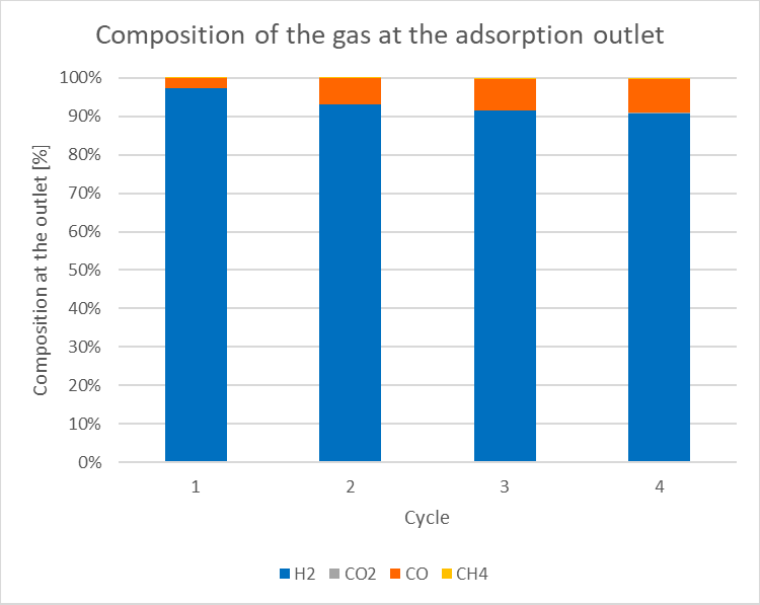

Figure 23. Composition of the gases at the adsorption outlet

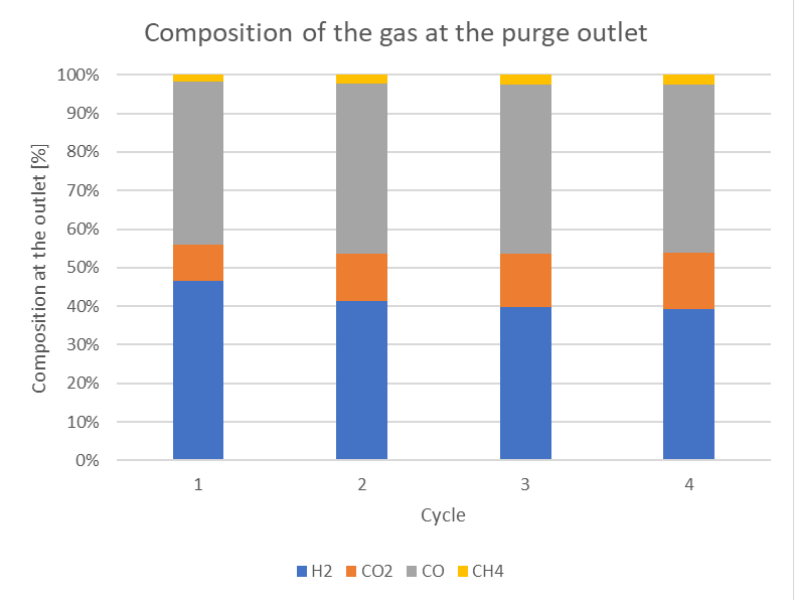

Figure 24. Composition of the gases at the purge outlet

The amount of CO and CO_2 is much higher in the purge phase: this is because these strongly adsorbed gases are later released back to the gas phase during the purge.

For the simulations, it has been chosen to use the purge ratio of 0.3: this means that 30% of the gas produced during the phase of adsorption is recirculated to the other column to regenerate it.

To double check the validity of the cycle patented by Skarström, simulations have been run with the co-current configuration. The result confirmed the reason why the other possible cycle is not used, as the selectivity of the material was shown to be lower and the adsorption curves had very low derivatives; particularly, the last slab was basically never regenerated. The choice of counter-current purge has been assessed as definitely better than the co-current flow.

4.2 Data from the simulations

In this subchapter are reported the data obtained in Excel in the simulations for all the cases; the simulation is interrupted once the quasi-steady state is reached.

1. **Case with raw gas, slow cycle and Carbon molecular sieve**

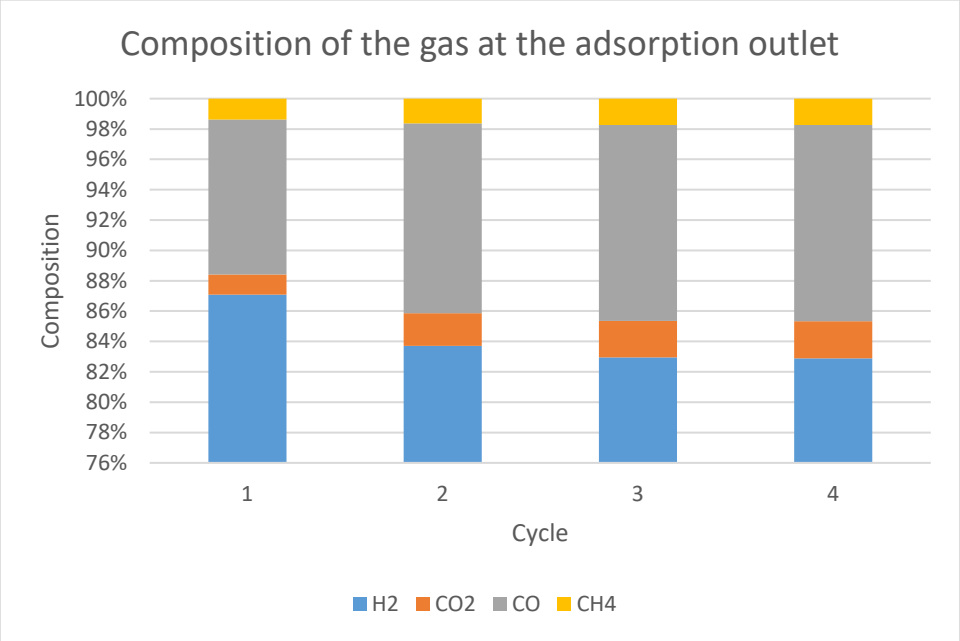

Figure 25. Composition of the gases at the outlet, in the case of raw gas, slow cycle and CMS

2. Case with raw gas, slow cycle and Activated carbon

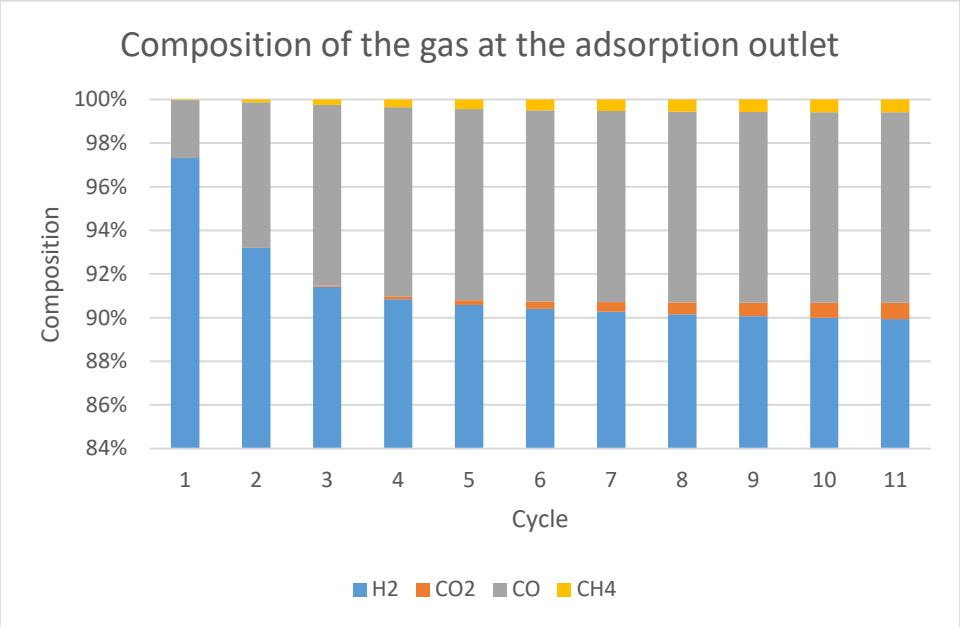

Figure 26. Composition of the gases at the outlet, in the case of raw gas, slow cycle and AC

3. Case raw gas, fast cycle and Carbon molecular sieve

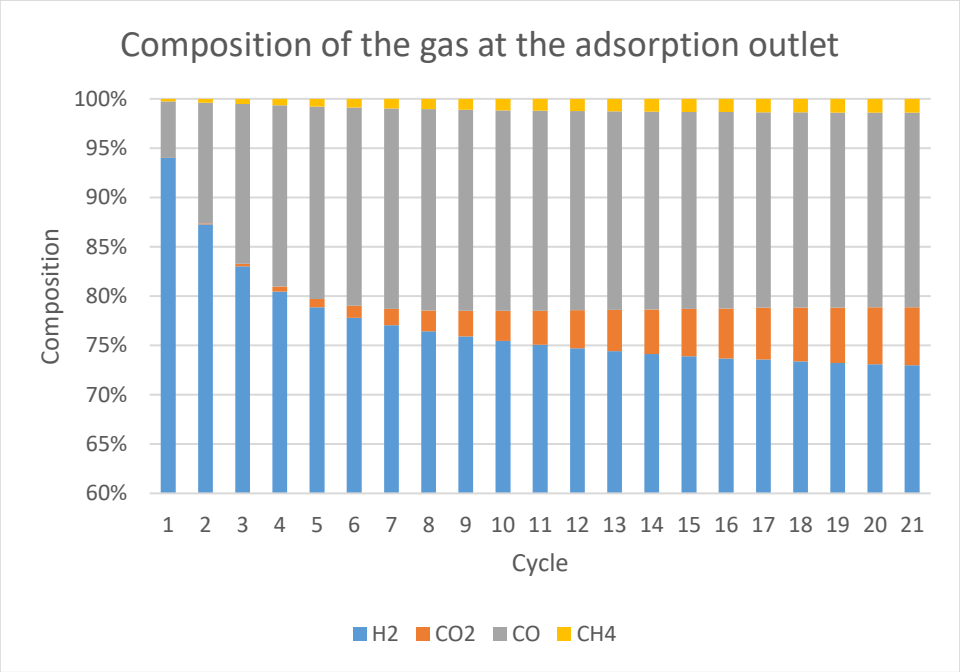

Figure 27. Composition of the gases at the outlet, in the case of raw gas, fast cycle and CMS

4. Case with raw gas, fast cycle and Activated carbon

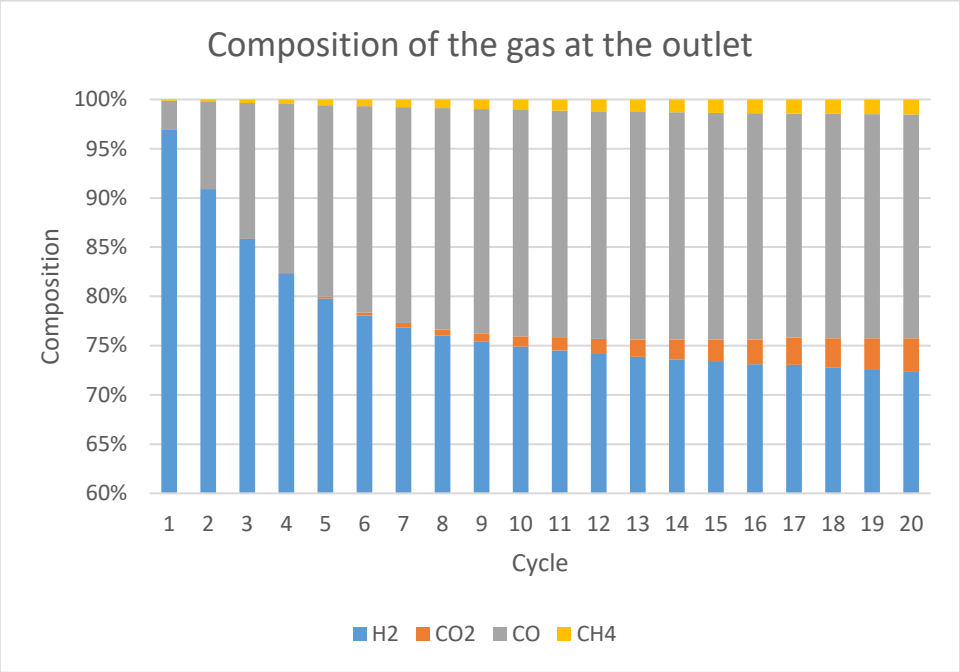

Figure 28. Composition of the gases at the outlet, in the case of raw gas, fast cycle and AC

5. Case with treated gas, slow cycle and Carbon molecular sieve

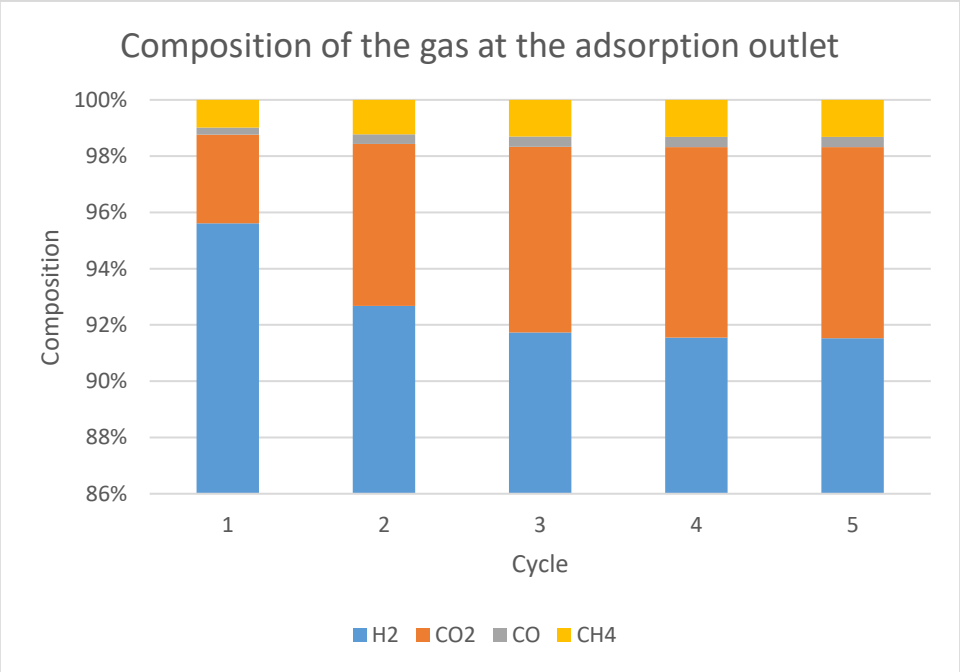

Figure 29. Composition of the gases at the outlet, in the case of treated gas, slow cycle and CMS

6. Case with treated gas, slow cycle and Activated carbon

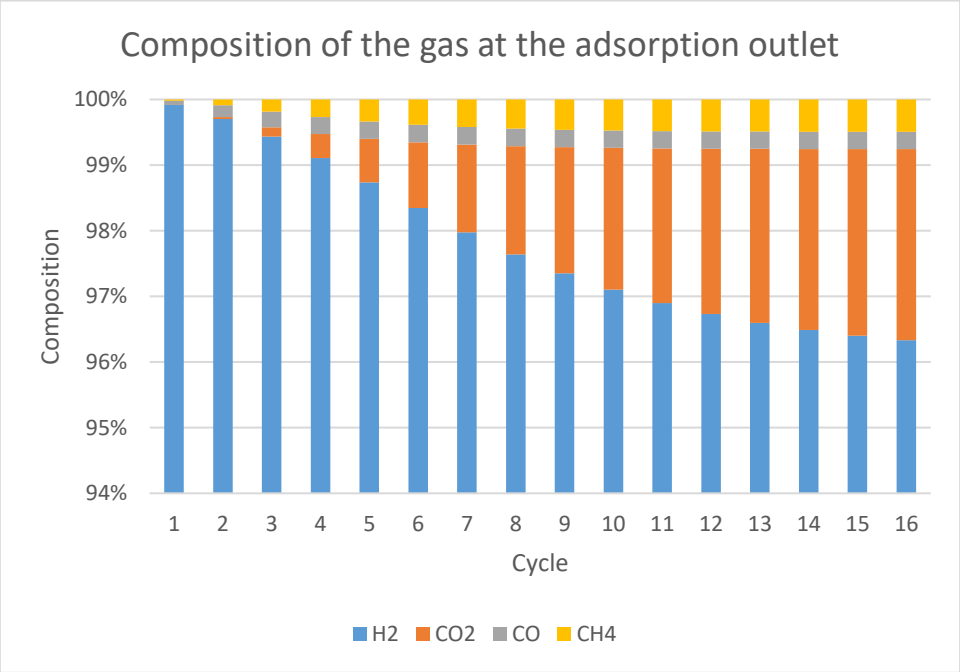

Figure 30. Composition of the gases at the outlet, in the case of treated gas, slow cycle and AC

7. Case with treated gas, fast cycle and Carbon molecular sieve

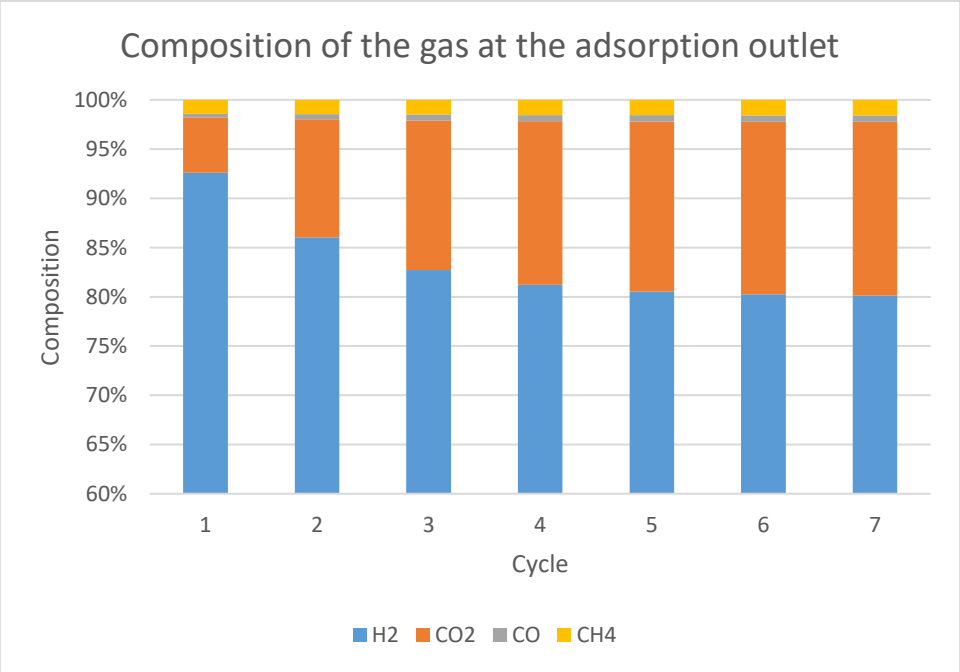

Figure 31. Composition of the gases at the outlet, in the case of treated gas, fast cycle and CMS

8. Case with treated gas, fast cycle and Activated carbon

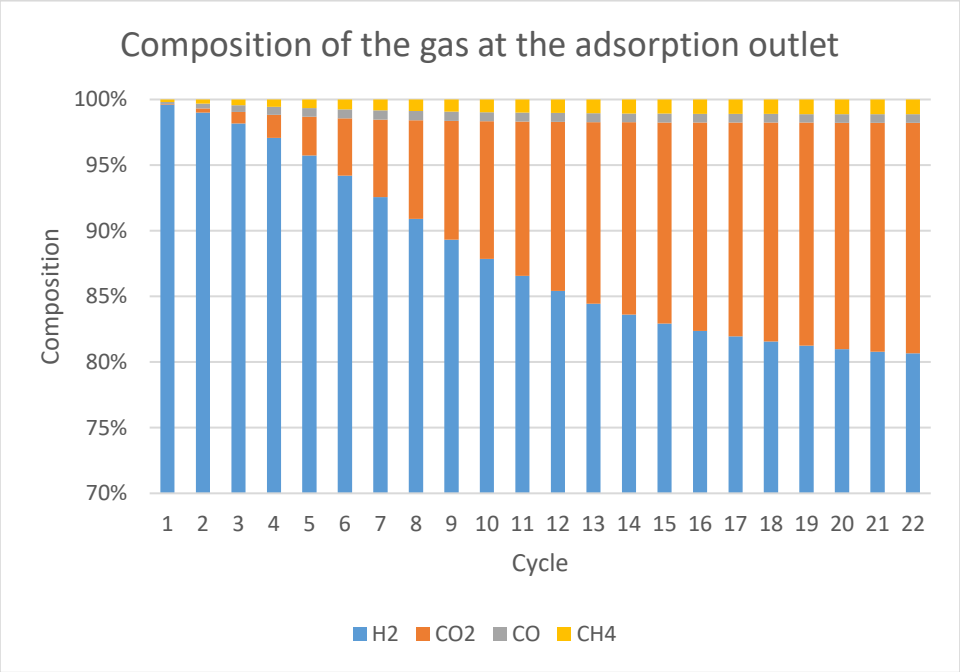

Figure 32. Composition of the gases at the outlet, in the case of treated gas, fast cycle and AC

5 Discussion

5.1 Results from the simulations

The results that have been obtained from the simulations, shown in Chapter 4 as columns, are reported in Table 9. The first four columns of the table show the composition of the gas at the outlet of the adsorption phase, while the column on the right is showing the number of cycles that took the simulation to reach the quasi-steady state. The quasi-steady state is reached when the composition of the gas changes less than 0,1% compared to the previous cycle; the usual figure that is used is 1%, but the choice of 0.1% makes the result more certain [54].

The results shown are the combinations of many factors, of which the most important is the selectivity of the adsorbent in relation to a target gas.

Table 9. Table summing up the values found in the simulations

Setting	Purity reached at QSS				Cycles before QSS
	H_2	CO_2	CO	CH_4	
Raw gas, slow cycle and CMS	82.9	2.4	12.9	1.7	4
Raw gas, slow cycle and AC	89.9	0.7	8.7	0.6	11
Raw gas, fast cycle and CMS	73.0	5.9	19.7	1.4	21
Raw gas, fast cycle and AC	72.3	3.4	22.7	1.5	20
Treated gas, slow cycle and CMS	91.5	6.8	0.4	1.3	5
Treated gas, slow cycle and AC	96.3	2.9	0.3	0.5	16
Treated gas, fast cycle and CMS	80.1	17.7	0.6	1.6	7
Treated gas, fast cycle and AC	80.7	17.6	0.6	1.1	22

The use of a slow cycle allows, in every case, to get a better purity of the gas, since the adsorbent is charged optimally and later releases the adsorbed gas. The use of a fast cycle does not exploit the desorption enough, since the material can never be properly regenerated. In the case of treated gas, fast cycle and Activated Carbon – thus in the case with a high percentage of CO_2 in the feed and the use of a material that can adsorb a high quantity of CO_2 – the situation resulted in a continuous adsorption but in a difficult desorption. The high number of cycles that were needed to reach the quasi-steady state is a consequence of this fact.

The Activated Carbon has an excellent behavior in relation to CO_2: in fact it can adsorb about double as much carbon dioxide in comparison to the Carbon Molecular Sieve. The best hydrogen purity overall was achieved by the Activated Carbon with the treated gas, and the use of a slow cycle. In this case, the purity reached was above 95%, which is a purity required in some industrial applications. It is suggested to use Activated Carbon in processes of separation that involve high amounts of CO_2, but the cycle has to be timed properly in such a way that the high amount of adsorbed material can properly be discharged. In general, for this type of application the Activated Carbon has shown to have a better performance overall: the Carbon Molecular Sieve performs

slightly better in relation to carbon monoxide, but the difference is not as wide as the cases with treated gas, in which the Activated Carbon is greatly better.

The usual setup used by PSA manufacturers is to use a specific adsorbent for every type of target gas, and then blend them together in the adsorption column or organize them in layers. The combined use of Activated Carbon in order to reduce the amount of CO_2, followed by Carbon Molecular Sieve to target carbon monoxide should be considered for a further study.

Unfortunately, the level of purity required for fuel cell applications has not been reached by any run of the simulation. This is due to a number of reasons, between which the main ones that have to be cited are:

- The simulation software was not specific for the chemical background, and many phenomena have been neglected, such as the real mechanisms of adsorption and the diffusion effects.
- The LDF constants were estimated for the particular case but were not exactly related to the particular coupling of materials and gases
- The basic Skarström cycle is a simple setup that has been developed at the beginning of the use of PSA and is thus lacking many developments that increase the quality of the gas produced. To be more effective, the number of phases could be increased and improved, introducing pressure balancing steps between the columns. As well, the purge velocity is very low, and it is the feature that affected the most the regeneration of the adsorbent. A higher purge velocity in the flow should be considered, together with a longer purge time compared to the adsorption time.

During the research time, multiple suppliers have been contacted, including one of the market leaders and a research center, and the feasibility of the syngas cleaning process has been reported as positive. Moreover, reaching the limits set by the manufacturer Powercell (25 ppm of CO) is not particularely problematic, while, using particular types of adsorbents, the purity required for automotive fuel cells (0,2 ppm CO) can be reached too.

The technical side of the solution implemented by the manufacturer was that the adsorption was carried out on 9 beds, timed between each other and optimized to target the exact gas composition [59].

5.2 P&ID of the solution

The Piping and Instrumentation Diagram – or P&ID - is an extremely important step in order to effectively design and structure a system that involves pipes and fluids that need to be treated under particular conditions.

The main aim of this type of design is to show the connections between the different items present in the system and their function in the process; the P&ID is the development that comes after the design of the Process Flow Diagram, that shows the general connections between blocks and the names of the reactors, without going in the detailed description of the control systems. The drawing contains all the main mechanical and process components of the systems that are mainly valves and instrumentation; the media contained in the system can be marked with different colors, especially in the case there are multiple flows taking part in the reaction.

The usual phases of the design of an installation are:

- Process flow diagram
- Piping and Instrumentation Diagram – Basic design
- Piping and Instrumentation Diagram – Detailed design

Once the Basic design is completed, the Hazard and Operability study – HAZOP – is performed. This study is considering all the safety issues that come up during the operation, the start-up and the shut-down. Once this study is completed, the detailed design is produced, from which all the important parameters for the actual commissioning of the plant can be calculated, such as the length and the diameter of the pipes or the size of the installation.

The aim of the design done for this thesis is to produce a Basic Design P&ID, in such a way that the main components to be purchased are known, and a first cost estimation could have been done. HAZOP has not been performed, although it has been discussed with some Cortus's responsibles for the safety of the plant regarding the quality of the P&ID designed and has harvested many suggestions in how to have a reliable and realistic system.

The P&IDs are shown in the first Appendix: the first case without recirculation and the second case with a double stage PSA.

5.3 Cost estimation for the installation

The possible application of the system has also to consider the practical costs that the installation of the system in the test plant would mean for the company. The Piping and Instrumentation Diagrams have been the base for the estimations of these costs.

The price of components has been estimated using quotes of items already purchased by Cortus for similar projects: this has been useful in regard to general piping engineering items, such as hand valves and other control valves. The cost of the main components of the system (i.e. the PSA and the fuel cell) has been estimated using the quotes given directly by the manufacturing companies. In general, it is possible to find two different types of items to be purchased: the general piping instruments, such as hand valves, are quite universal for any system; on the other hand, the assemblies, such as the PSA or the Water-gas Shift, are sold in a block together with other control instruments (such as sensors) and have a price that reflects the whole. For this reason, some valves that can be found inside the assemblies were not counted in the matter of the total budget estimation.

The systems that need a connection with the PLC (the plant's computer), have a higher purchase cost but are also a further expense in the system, as they need to be installed by specialized personnel and programmed. These components are typically the sensors, the control valves, and the safety circuit equipment.

As it can be noticed by the following tables, the cost of components is very relevant in the total cost of the system. This is due to the high purchase cost of the PSA and the fuel cell system, that alone weigh about 80% of the total estimated cost of the system.

The design of the system and its installation represent the two other major costs: the first figure consists of the work that has to be done to develop the first draft of P&IDs, in order to select the components to purchase, together with the safety analysis (HAZOP); the second one is the physical installation of the components on site and its connection to the PLC.

The first part of the work is done in the office, in which the preliminary study with a P&ID is done, and the estimation of the component cost is completed. With that, a 3D model is prepared and the fitting in the existing plant is assessed; later on, the purchase of the items has to be managed: the potential suppliers have to be contacted and requested quotes that need to be processed in order to choose the best supplier.

After that, the electrical and mechanical installations can be completed on-site: once the components have reached the test site, they can be mounted and connected to the PLC (the Programmable Logic Controller, the plant's computer). The whole system will be eventually manageable in remote via PLC.

5.3.1 System with single pass

The cost estimate for the linear system, in which the stream passes in every reactor one after another, is reported in this subchapter.

The major voice of cost for the system are its main components, namely the PSA unit and the fuel cell block. The price of these units is reported as the figure directly reported on the first quote sent by the supplier; no negotiation for the prices has taken place so far.

In Table 10 are reported the prices of the single components (present in the P&ID) for the system with a single pass. The figures listed are reported according to the most recent quotes from the suppliers available at the Company. The P&ID of this system can be found in the Appendix.

It has to be remarked how the price of automatic valves (thus every valve that needs to be controlled remotely) is way higher compared to the price of a mechanical device that does not need a signal to work. Moreover, an automatic valve needs to be connected to the electricity (or compressed air) circuit and programmed in the PLC. Table 11 is summing up all the purchasing costs and considers the installation costs too.

The costs are considered in Swedish Crowns, or SEK: the conversion rate of this currency during the year 2017 with Euro was 0.104 €/SEK, and this value has been used to calculate its equivalence in the European currency.

Table 10. Cost estimation of the components of the system in the linear configuration

Quantity	Component	Fluid	Price (SEK)	Total price
16	Hand valve DN15	Various	SEK 340.00	SEK 5,440.00
1	Non return valve	Niitrogen	SEK 500.00	SEK 500.00
5	Temperature transmitter	Various	SEK 1,632.00	SEK 8,160.00
3	0-15 barg	Various	SEK 6,000.00	SEK 18,000.00
2	Safety relief valve	Syngas	SEK 1,710.00	SEK 3,420.00
3	Vessels for the syngas storing	Syngas	SEK 1,000.00	SEK 3,000.00
1	Electric heater before the WGS	Syngas	SEK 1,800.00	SEK 1,800.00
1	Control valves on syngas, steam and water		SEK 20,000.00	SEK 20,000.00
1	Condensate trap	Syngas	SEK 2,600.00	SEK 2,600.00
1	Pressure reducing valve	Syngas	SEK 1,710.00	SEK 1,710.00
1	Air fan	Air	SEK 1,500.00	SEK 1,500.00
1	Strainer	Air	SEK 500.00	SEK 500.00
1	Compressor including cooler		SEK 50,000.00	SEK 50,000.00
1	WGS reactor, including the cooling heat exchanger		SEK 100,000.00	SEK 100,000.00
1	PSA including control and measuring systems		SEK 676,800.00	SEK 676,800.00
1	Fuel cells, including the control system		SEK 350,000.00	SEK 350,000.00
TOTAL				**SEK 1,243,430.00**

Table 11. Cost estimation of the installation of the linear configuration

Budget Estimation	
Components	SEK 1,243,430.00
Control system Design and Programming	SEK 66,000.00
Hardware (20% of D&P)	SEK 13,200.00
Electrical installation	SEK 36,000.00
Pipe and mechanical design	SEK 80,000.00
Mechanical installation	SEK 200,000.00
Purchase coordination	SEK 72,000.00
Subtotal	SEK 1,760,630.00
Miscellaneus 20%	SEK 352,126.00
SUM	**SEK 2,062,756.00**

As it is possible to notice by Table 11, the installation cost is as well very relevant in respect of the total cost of the system. This is due to the high number of components, that make the installation longer and more complicated, both from the mechanical and from the engineering point of view. In fact, the components have to be engineered at the office level, and then have to be actually commissioned in the plant. The phase of commissioning means the mechanical work involved in welding and mounting the components and the electrical installation considers the connection of the systems that require a signal to the PLC.

Using the average exchange rate as in October 2017, the total cost of the unit in Euros would be €215,000, with the rate being about 0.104 €/SEK.

5.3.2 System with double pass

The cost estimation of the system with a double PSA pass, considering the treatment of the raw gas and the further processing of the off-gas through the treatment in a second PSA, has been reported. This configuration differs from the first one in the presence of one more compressor unit and one more PSA assembly. The number of components is higher, and the capital cost for this installation is thus rising too, of roughly 50%.Another issue that might be taken into consideration is the possibility of more failures in the system, that would need to be assessed in a HAZOP analysis. The P&ID of this solution can be found in the Appendix.

Table 12. Cost estimation of the components of the system in the recirculation configuration

Quantity	Component	Fluid	Price (SEK)	Total price
18	Hand valve DN15	Nitrogen	SEK 340.00	SEK 6,120.00
2	Non return valve	Various	SEK 500.00	
4	TT 0-100°C	Various	SEK 1,632.00	SEK 6,528.00
1	TT 0-500°C	Syngas	SEK 1,632.00	SEK 1,632.00
3	0-15 barg	Various	SEK 6,000.00	SEK 18,000.00
3	Safety relief valve	Syngas	SEK 1,710.00	SEK 5,130.00
3	Vessels for the syngas storing	Syngas	SEK 1,000.00	SEK 3,000.00
1	Electric heater before the WGS	Syngas	SEK 1,800.00	SEK 1,800.00
1	Control valve on the WGS		SEK 20,000.00	SEK 20,000.00
1	Condensate trap	Syngas	SEK 2,600.00	SEK 2,600.00
2	Pressure reducing valve	Syngas	SEK 1,710.00	SEK 3,420.00
1	Air fan	Air	SEK 1,500.00	SEK 1,500.00
1	Strainer	Air	SEK 500.00	SEK 500.00
2	Compressor including cooler		SEK 100,000.00	SEK 200,000.00
1	WGS reactor, including the cooling heat exchanger		SEK 100,000.00	SEK 100,000.00
2	PSA including control and measuring systems		SEK 676,800.00	SEK 1,353,600.00
1	Fuel cells, including the control system		SEK 350,000.00	SEK 350,000.00
TOTAL				**SEK 2,022,198.00**

Table 13. Cost estimation of the installation of the recirculation configuration

Budget Estimation	
Components	SEK 2,022,198.00
Control system Design and Programming	SEK 87,000.00
Hardware (20% of D&P)	SEK 17,400.00
Electrical installation	SEK 36,000.00
Pipe and mechanical design	SEK 80,000.00
Mechanical installation	SEK 250,000.00
Purchase coordination	SEK 90,000.00
Subtotal	SEK 2,632,598.00
Miscellaneus 20%	SEK 526,519.60
SUM	**SEK 3,109,117.60**

The same remarks stated for the linear configuration can be said for the system with recirculation: the high number of components, and the high amount of commissioning work that needs to be done to complete the unit leads the mechanical and electrical installation cost to be very high. Table 13 reports all the costs for a possible installation.

Using the average exchange rate as in October 2017, the total cost of the unit in Euros would be €325,000, with the rate being around 0.104 €/SEK.

6 Conclusions

This work has analyzed the purification of a syngas stream coming from biomass gasification through the WoodRoll® process for the production of hydrogen for fuel cell specifications.

A state of the art review has been presented, with the solutions that are usually present in the industrial environment for similar plant setups; a review of the reaction of water-gas shift and the purification methods has been presented. The main models that describe adsorption, such as Langmuir, BET and Henry's have been presented, to give a mathematical basis to the phenomenon; a review of fuel cells and their requirements is given at the end of the state of the art. The choice of the system setup has been a combination of a water-gas shift reactor with a PSA – Pressure Swing Adsorption unit. The system could be developed into two different setups: one possibilities leads all the stream in a reactor after another, while another possibility is to use a double pass into a PSA, in order to have a higher yield in the Water-gas shift reaction and to have the possibility of producing gas with different blending of hydrogen and CO.

Simulations on the model developed have been run according to Langmuir model and using Euler's method to solve the system of partial differential equations that describe the behavior of a phenomenon in an adsorption column. The choice has been to use different combinations of parameters. The variables changed have been the different adsorbing material, the duration of the adsorption cycle and the composition of the gas, considering whether it was previously treated through a WGS or not. The results of these simulations are presented in Chapter 4. The use of Activated Carbon has shown interesting results, because of its high capacity of adsorbing carbon dioxide. Specifically, the best result obtained – in quasi-steady state configuration – has been of a purity of 96.3% of H_2 and 0.3% of CO. The purity for fuel cells specifications has not been reached, but the causes of that were supposed to be in the model, that uses many approximations, in the not optimized cycle for the specifics of this gas, and in the LDF constants that were hypothesized.

A piping and instrumentation diagram - P&ID – has been prepared for the two different setups, and it can be found integrally in the Annex. Using the two P&IDs, two cost estimations for the complete installation of the unit have been performed. The two different configurations have shown to have a very different capital cost, with the solution with double pass resulting in a higher expense. The configuration with a single pass was estimated to cost 2,1 million Swedish crowns, while the configuration with a double PSA pass was estimated to cost 3,1 million SEK, considering all the projecting and installation costs. However, a detailed cost-benefit analysis should be performed to state which system to choose should be performed.

The purity required by modern fuel cells requires a demanding purification process, but it is achievable and, by investigating the feasibility with suppliers, it has been found that it is reachable with an optimization of the system and the use of high-quality adsorbents.

7 References

[1] L. Mehe, D. Sagar and S. Naik, "Technical aspects of biodiesel production by transesterification - A review," *Renewable and Sustainable Energy Reviews,* vol. 10, no. 3, pp. 248-268, 2006.

[2] C. R. Hammond, "The Elements," in *Handbook of Chemistry and Physics 81st ed.*, Boca Raton, FA, USA, CRC Press, 1997.

[3] IEA - International Energy Agency, "Hydrogen Production & Distribution," IEA Energy Technology Essentials, 2007.

[4] J. Rifkin, The Hydrogen Economy, New York, USA: Penguin, 2003.

[5] Cortus Energy, "WoodRoll® - a flexible and robust gasification technology with extraordinary performance," Cortus Energy AB, Stockholm, Sweden, 2014.

[6] T. Ramsden and D. Steward, "Analyzing the Levelized Cost of Centralized and Distributed Hydrogen Production Using the H2A Production Model, Version 2," National Renewable Energy Laboratory, USA, Golden, CO, USA, 2009.

[7] Z. Barlow, "Breakthrough in hydrogen fuel production could revioutionize alternative enrgy market," Virginia Tech News, 2013.

[8] PATH - Partnership for Advancing the Transition to Hydrogen, "Annual Report on World Progress in Hydrogen," 2011.

[9] K. Liu, C. Song and V. Subramani, Hydrogen and Syngas production and purification technologies, Hoboken, New Jersey: Wiley, 2010.

[10] W. Vielstich, A. Lamm and H. A. Gasteiger, Handbook of fuel cells: fundamentals, technology, applications, New York: Wiley, 2003.

[11] Stepwise project, "Stepwise project," 05 09 2017. [Online]. Available: http://www.stepwise.eu/project/. [Accessed 05 09 2017].

[12] A. Golmakani, S. Fatemi and J. Tamnanloo, "Investigating PSA, VSA, and TSA methods in SMR Unit of Refineries for Hydrogen production for FC specification," *Separation and Purification technology,* vol. 176, pp. 73-91, 2016.

[13] C. W. Skarström, "Method and apparatus for fractionating gaseous mixtures by adsorption". USA Patent 2944627, 07 12 1960.

[14] C. Siettos, "Enabling dynamic process simulators to perform alternative tasks: a time-stepper-based toolkit for computer aided analysis," Industrial Engineering Chemical Resources, 2003.

[15] A. Rudelstorfer and E. Fuderer, "Selective Adsorption of Gases". USA Patent 3,986,849, 1976.

[16] P. L. Cen, W. N. Chen and R. T. Yang, "Ternary gas mixture separation by Pressure Swing Adsorption: a combined hydrogen-methane separation and acid gas removal," *Ind. Eng. Chem. Process Des. Dev.,* vol. 24, no. 4, pp. 1201-1208, 1985.

[17] Britannica, Encyclopaedia, "Adsorption," in *Encyclopaedia Britannica*, Edimburgh, Scotland, Encyclopaedia Britannica, 1998.

[18] G. Sposito, The chemistry of soils, Oxfod, England: Oxford University Press, 1989.

[19] K. Sing and e. al., "Reporting physisorption data for gas/solid systems," *Pure & Appl. Chem.,* vol. 57, no. 4, pp. 603-619, 1985.

[20] A. Trunschke, "Surface area and Pore size determination," in *Moden Methods in Heterogeneous Catalysis Research*, Berlin, 2013.

[21] J. Gibbs, Collected Works, New Have, Connecticut, USA: Yale University Press, 1928.

[22] D. M. Ruthven, Principles of Adsorption and Adsorption Processes, New York: John Wiley & Sons, 1984.

[23] S. Goldberg, "Adsorption Models Incorporated into Chemical Equilibrium Models," *Chemical Equilibrium and Reaction Models,* no. Special publication 42, pp. 75-95, 1995.

[24] J. W. Bain, The sorption of Gases and Vapours by Solids, London: Routledge, 1932.

[25] W. Henry, Experiments on the quantity of gases absorbed by water, at different temperatures, and under different pressures, London: Phil. Trans. R. Soc. Lond, 1803.

[26] A. H. Berger and A. S. Bhown, "Comparing Physisorption and Chemisorption Solid Sorbents for use Separating CO2 from Flue Gases using TSA," *Energy Procedia,* vol. 4, pp. 562-567, 2011.

[27] M. Annesini, R. Augelletti, M. De Falco and S. Frattari, "Production and purification of hydrogen-methane mixtures utilized in internal combustion engines," *Sustainable Development and Planning,* vol. 7, pp. 535-546, 2015.

[28] I. Langmuir, *The Adsorption of Gases on Plane Surface of Glass, Mica and Platinum,* vol. 40, The Research Laboratory of The General Electric Company, 1918.

[29] M. Manabu, F. Yuichi and Y. Katsunori, "Pure silica CHA type zeolite for CO2 separation using PSA ad high pressure," no. 38, 2012.

[30] Micrometrics Instrument Company, "Gas Adsorption Theory," Micrometitics Instrument Corporation, [Online]. Available: http://www.micromeritics.com/Repository/Files/Gas_Adsorption_Theory_poster.pdf. [Accessed 15 03 2017].

[31] S. Brunauer, L. Deming and W. Deming, "On a Theory of the van der Waals Adsorption of Gases," *J. Am. Chem. Soc.,* vol. 62, no. 7, pp. 1723-1732, 1940.

[32] L. L. Schramm, The Language of Colloid and Interface Science, American Chemical Society, 1993.

[33] I. Mostinsky, "Thermopedia - Adsorption," 03 02 2011. [Online]. Available: http://www.thermopedia.com/content/292/. [Accessed 13 03 2017].

[34] D. M. Ruthven, "Fundamentals of Adsorption Equilibrium and Kinetics in Microporous Solids," in *Adsorption and Diffusion. Molecular Sieves vol. 7*, Berlin, Heidelberg, Springer, 2008.

[35] H. Freudlich, "Over the adsorption in solution," in *J Phy. Chem.*, Washington, DC, ACS Publications, 1906, pp. 385-470.

[36] K. Y. Foo and B. H. Hameed, "Insights into the modeling of adsorption isotherm systems," *The Chemical Engineering Journal,* vol. 156, pp. 2-10, 2010.

[37] P. E. E. T. S. Brunauer, "On a Theory of the van der Waals Adsorption of Gases," *J. Am. Chem. Soc.,* vol. 60, no. 2, pp. 309-319, 1938.

[38] W. Yu and T. Patzek, "Modeling gas adsorption in Marcellus shale with Langmuir and BET isotherms," January 2016. [Online]. Available: https://www.researchgate.net/publication/289505424_Modeling_Gas_Adsorption_in_Marcellus_Shale_With_Langmuir_and_BET_Isotherms. [Accessed 12 04 2017].

[39] S. Sircar and J. Hufton, "Why Does the Linear Driving Force Model for Adsorption Kinetics Work?," *Adsorption,* vol. 6, pp. 137-147, 2000.

[40] A. A. Christy, "Quantitative determination of surface area of silica gel particles by near infrared spectroscopy and chemometrics," *Colloids and Surfaces: A Physicochemical and Engineering Aspects,* vol. 322, no. 1-3, pp. 248-252, 2008.

[41] A. F. Cronstedt, Stockholm: Kongl Vetenskaps Academiens Handlingar Stockholm, 1756.

[42] J. Newsam, "The Zeolite Cage Structure," *Science,* vol. 231, no. 4742, p. 1093, 1986.

[43] International Zeolite Association, "Database of Zeolite structures," International Zeolite Association, 2016.

[44] B. Smit and T. L. M. Maesen, "Molecular Simulations of Zeolites: Adsorption, Diffusion, and Shape Selectivity," *Chem. Rev.,* vol. 108, pp. 4125-4184, 2008.

[45] Encyclopaedia Britannica, "Fuel Cell," in *Encuclopaedia Britannica*, Edimburgh, Scotland, Encyclopaedia Britannica, 2017.

[46] 4th Energy Wave, "Fuel Cell Annual Report," 4th Energy Wave, 2015.

[47] R. Dervisoglu, "Fuel cell scheme," 07 12 2015. [Online]. Available: https://en.wikipedia.org/wiki/File:Solid_oxide_fuel_cell_protonic.svg. [Accessed 15 10 2017].

[48] J. Larminie and A. Dicks, Fuel Cell Systems Explained, Wiley, 2003.

[49] USF Learn, "USF Learn," [Online]. Available: https://usflearn.instructure.com/courses/986898/files/31116394. [Accessed 08 05 2017].

[50] Clean Power Solution Ltd., "The PEM Fuel Cell Market 2015-2019 Outlook," CPSL, 2015.

[51] Y. Wang, K. Chen, J. Mishler, S. C. Cho and X. C. Adroher, "A review of PEM fuel cells: Technology, applications, and needs on fundamental research," *Applied Energy,* vol. 88, no. 4, pp. 981-1007, 2011.

[52] M. K. Debe, "Advanced cathode catalysts and supports for PEM fuel cells," DOE Hydrogen Program Review, 2010.

[53] B. Axelberg, "Application of a Water-Gas shift reaction to the WoodRoll process," Master thesis for KTH, Stockholm, 2017.

[54] J. Kim and S. Young, "Study on a numerical model and PSA (pressure swing adsorption) process experiment for CH4/CO2 separation from biogas," *Energy - The International Journal,* vol. 91, pp. 732-741, 2015.

[55] D. M. Ruthven, S. Farooq and K. Knaebel, Pressure Swing Adsorption, New York: VCH Publishers, Inc., 1994.

[56] J. Rother and T. Fieback, "Multicomponent adsorption measurements on activated carbon, zeolite molecular sieves and metal-organic framework," *Adsorption - Journal of the Adsorption Society,* vol. 19, pp. 1065-1074, 2013.

[57] Carbotech GmbH, *Carbotech technical brochure,* 2017.

[58] TIGG Corporation, "Catalogs and Brochures," 2012. [Online]. Available: http://tigg.com/TIGG-corporate-catalog-brochures.html. [Accessed 15 10 2017].

[59] Xebec Inc., *Budget Proposal for Xebec G1 PSA unit,* Blainville, Canada, 2017.

Appendix

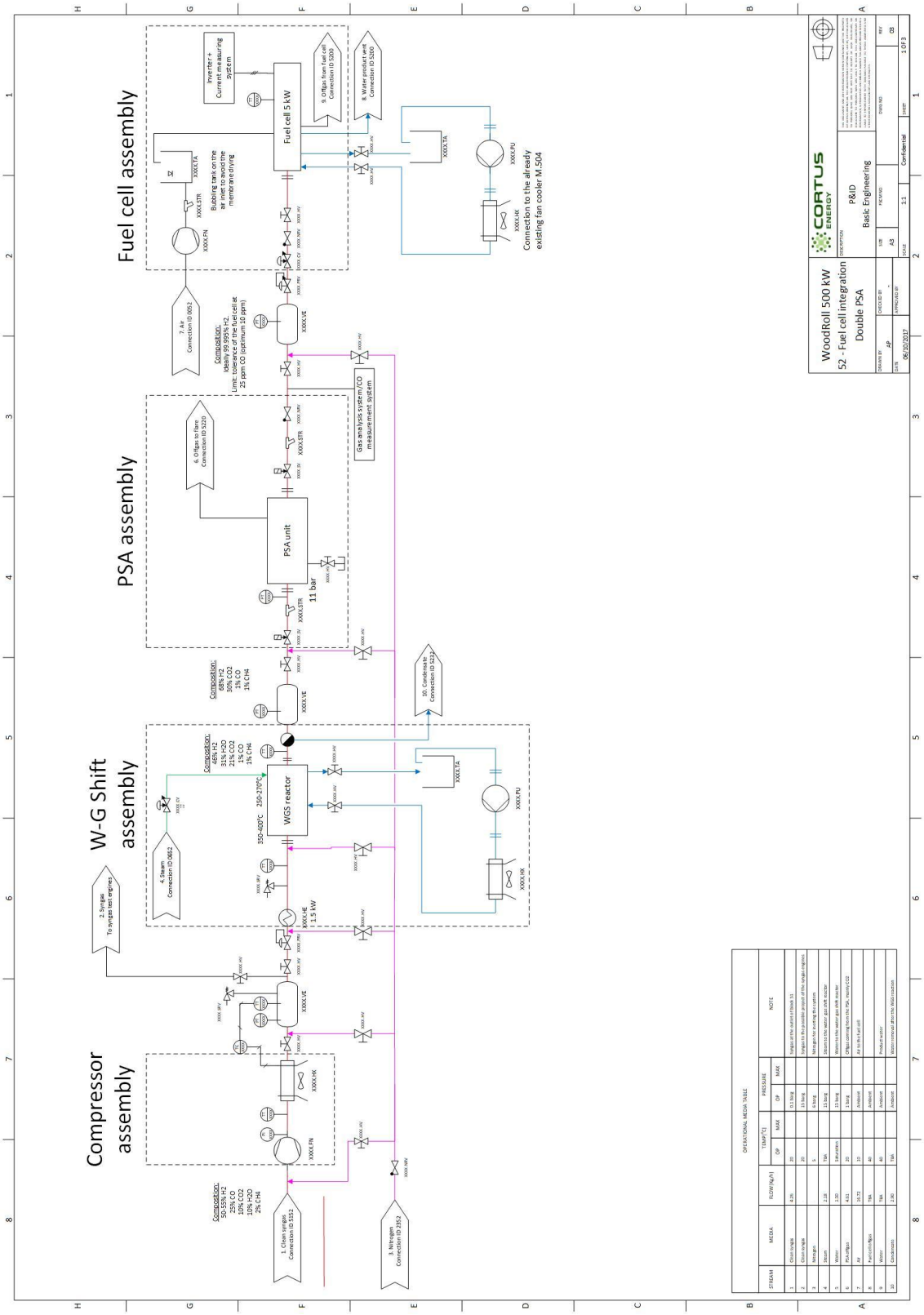
Compressor assembly
W-G Shift assembly
PSA assembly
Fuel cell assembly
WGS reactor
PSA unit
Fuel cell 5 kW
Connection to the already existing fan cooler M.504
WoodRoll 500 kW
52 - Fuel cell integration
Double PSA
P&ID
Basic Engineering
CORTUS ENERGY
Confidential

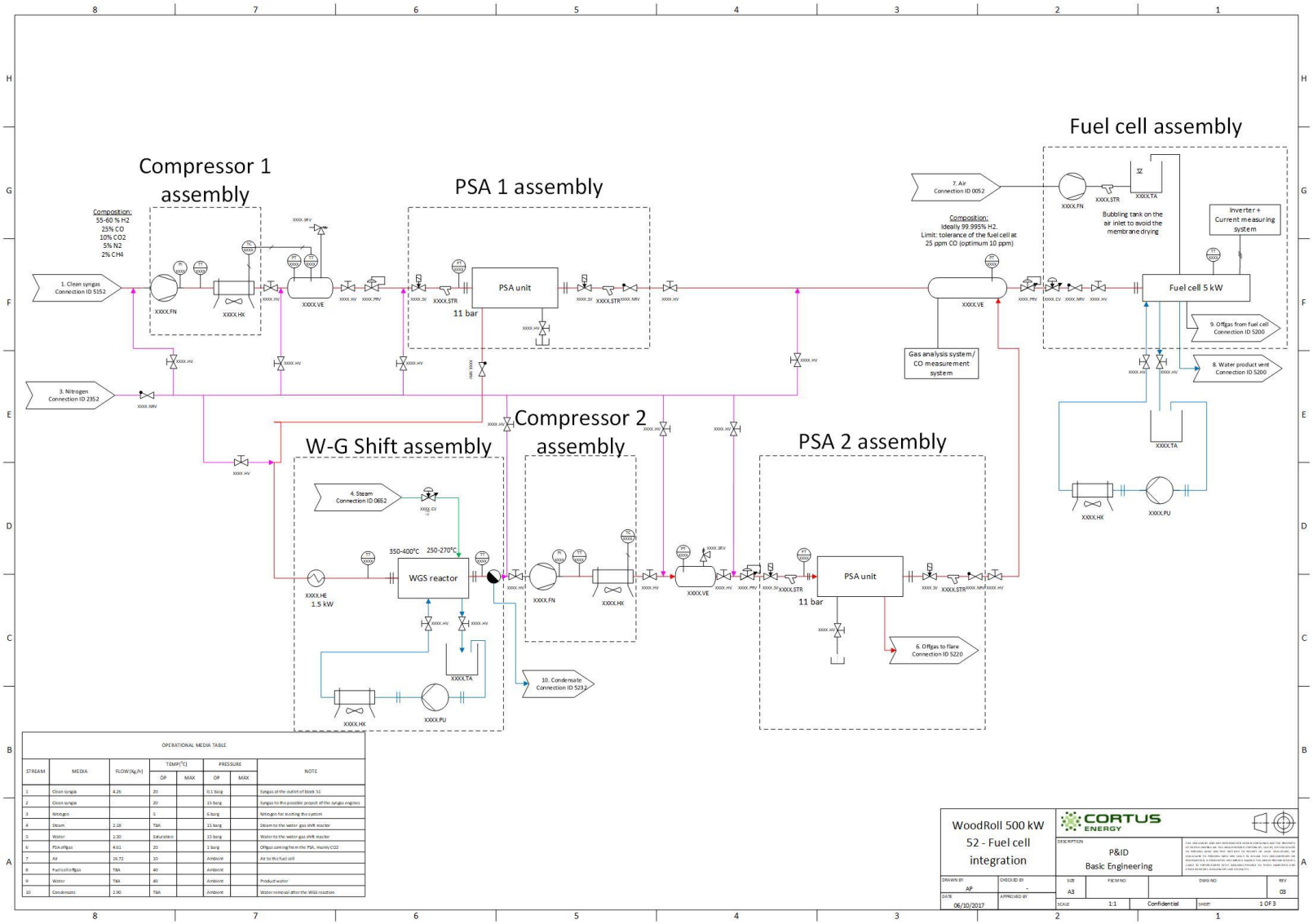

OPERATIONAL MEDIA TABLE

STREAM	MEDIA	FLOW [Kg/h]	TEMP [°C] OP	TEMP [°C] MAX	PRESSURE OP	PRESSURE MAX	NOTE
1	Clean syngas	4.26	20		0.1 barg		Syngas at the outlet of block 31
2	Clean syngas		20		15 barg		Syngas to the possible project of the syngas engines
3	Nitrogen		5		6 barg		Nitrogen for starting the system
4	Steam	2.18	TBA		15 barg		Steam to the water gas shift reactor
5	Water	1.30	Saturation		15 barg		Water to the water gas shift reactor
6	PSA offgas	4.61	20		1 barg		Offgas coming from the PSA, mainly CO2
7	Air	16.72	20		Ambient		Air to the fuel cell
8	Fuel cell offgas	TBA	40		Ambient		
9	Water	TBA	40		Ambient		Product water
10	Condensate	2.90	TBA		Ambient		Water removal after the WGS reaction

WoodRoll 500 kW 52 - Fuel cell integration	CORTUS ENERGY		
	DESCRIPTION: P&ID Basic Engineering		
DRAWN BY: AP	CHECK ID BY: -	SIZE: A3	FICM NO:	DWG NO:	REV: 03
DATE: 06/10/2017	APPROVED BY:	SCALE: 1:1	Confidential	SHEET: 1 OF 3	